

REPORT DOCUMENTATION PAGE

Form Approved
OMB No. 0704-0188

Public reporting burden for this collection of information is estimated to average 1 hour per response, including the time for reviewing instructions, searching existing data sources, gathering and maintaining the data needed, and completing and reviewing the collection of information. Send comments regarding this burden estimate or any other aspect of this collection of information, including suggestions for reducing this burden, to Washington Headquarters Services, Directorate for Information Operations and Reports, 1215 Jefferson Davis Highway, Suite 1204, Arlington, VA 22202-4302, and to the Office of Management and Budget, Paperwork Reduction Project (0704-0188), Washington, DC 20503.

AD-A224 688

1. AGENCY USE ONLY (Leave blank)		2. REPORT DATE 1990	3. REPORT TYPE AND DATES COVERED Thesis/Dissertation	
4. TITLE AND SUBTITLE REGULATION OF GLUTATHIONE IN A RAT DIPLOID HEPATIC EPITHELIAL CELL LINE			5. FUNDING NUMBERS	
5. AUTHOR(S) STEPHEN R. CHANNEL				
7. PERFORMING ORGANIZATION NAME(S) AND ADDRESS(ES) AFIT Student at: University of Washington			8. PERFORMING ORGANIZATION REPORT NUMBER AFIT/CI/CIA - 90-054	
9. SPONSORING/MONITORING AGENCY NAME(S) AND ADDRESS(ES) AFIT/CI Wright-Ptatterson AFB OH 45433			10. SPONSORING/MONITORING AGENCY REPORT NUMBER	
11. SUPPLEMENTARY NOTES				
12a. DISTRIBUTION/AVAILABILITY STATEMENT Approved for Public Release IAW AFR 190-1 Distribution Unlimited ERNEST A. HAYGOOD, 1st Lt, USAF Executive Officer, Civilian Institution Programs			12b. DISTRIBUTION CODE	
13. ABSTRACT (Maximum 200 words)				
<p>DTIC SELECTED AUG 1 1990 S B D</p>				
Original contains color plates: All DTIC reproductions will be in black and white				
14. SUBJECT TERMS			15. NUMBER OF PAGES 114	16. PRICE CODE
17. SECURITY CLASSIFICATION OF REPORT UNCLASSIFIED	18. SECURITY CLASSIFICATION OF THIS PAGE	19. SECURITY CLASSIFICATION OF ABSTRACT	20. LIMITATION OF ABSTRACT	

Regulation of Glutathione
in a Rat Diploid Hepatic
Epithelial Cell Line

by

Stephen R. Channel

A thesis submitted in partial fulfillment
of the requirements for the degree of

Master of Science

University of Washington

1990

Approved by *David L. Eaton*
(Chairperson of Supervisory Committee)
James H. ...
Elaine M. Faustman

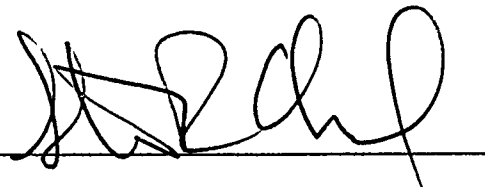
Program Authorized to Offer Degree Public Health and Community Medicine

Date 4 Jun 90

Master's Thesis

In presenting this thesis in partial fulfillment of the requirements for a Master's degree at the University of Washington, I agree that the Library shall make its copies freely available for inspection. I further agree that extensive copying of this thesis is allowable only for scholarly purposes, consistent with "fair use" as prescribed in the U.S. Copyright Law. Any other reproduction for any purposes or by any means shall not be allowed without my written permission.

Signature

A handwritten signature in black ink, appearing to be "J. R. [unclear]", written over a horizontal line.

Date

4 Jun 90

TABLE OF CONTENTS

	Page
List of Figures	iii
List of Tables	v
Introduction	1
Glutathione Synthesis	1
Glutathione Metabolism/Utilization	5
Cell Culture	8
Materials and Methods	16
Chemicals	16
Cell Culture and Harvest	17
Growth and DNA	17
Flow Cytometric Analysis	18
Immunohistochemistry	19
Uridine/Leucine Uptake	21
HPLC Assay	22
ELISA Assay	25
CDNB Assay	29
GSH Depletion/Repletion	29
BrDU Cell Cycle Method	30
Data Analysis	32
Results	33
Morphology	33
Growth and DNA	34
Albumin/Fetal Protein Expression	34
GST and γ GCS Induction	35
Depletion/Repletion Studies	39
Discussion	92
WB344 Characterization	92
Induction of γ GCS	92
Depletion and Repletion of GSH	94
Cycloheximide Effect	98
Conclusions	102
References	105

Accession For	
NTIS GRA&I	<input checked="" type="checkbox"/>
DTIC TAB	<input type="checkbox"/>
Unannounced	<input type="checkbox"/>
Justification	
By _____	
Distribution/	
Availability Codes	
Dist	Avail and/or Special
A-1	



LIST OF FIGURES

Number	Page
1. GSH biosynthesis/metabolism	13
2. Cellular transport systems	14
3. WB344, subconfluent, no stain	47
4. WB344, subconfluent, H&E	48
5. WB344, cell islands, H&E	49
6. WB344, early confluence	50
7. WB344, confluence, H&E	51
8. WB344, confluence, H&E, 400X	52
9. Log cell no. vs. time	53
10. Log cell no. vs. protein	54
11. DAPI DNA analysis	55
12. Albumin, WB344	56
13. AFP, WB344	57
14. Vimentin, WB344	58
15. Albumin, DES treated WB344	59
16. AFP, DES treated WB344	60
17. Vimentin, DES treated WB344	61
18. Phenobarbital - GST isozymes	64
19. GST profile - cytosol standard	65
20. GST profile - phenobarbital	66
21. BHA - GST isozymes	67
22. GST profile - BHA	68
23. Selenium - GST isozymes	69
24. GST profile - selenium	70

25. GSH overshoot	71
26. ACD effect on GSH overshoot	72
27. CYC effect on GSH overshoot	73
28. GSH recovery following BSO	74
29. ACD effect on GSH recovery	75
30. CYC effect on GSH recovery	76
31. Effect of 500 μ M BSO	77
32. CYC effect on BSO inhibition	78
33. Acivicin effect on CYC elevation of GSH . . .	79
34. CYC-mediated GSH increase	80
35. Control cell profile - 12 hours	82
36. CYC cell cycle profile - 12 hours	83
37. Control cell profile - 20 hours	84
38. CYC cell cycle profile - 20 hours	85
39. Control cell profile - 28 hours	86
40. CYC cell cycle profile - 28 hours	87
41. Control cell profile - 36 hours	88
42. CYC cell cycle profile - 36 hours	89
43. Control cell profile - 48 hours	90
44. CYC cell cycle profile - 48 hours	91
45. CYC structure/possible mechanisms	104

LIST OF TABLES

Number	Page
1. Phenotypic Profiles	15
2. Induction of γ GCS in WB344	62
3. Induction of GST in WB344	63
4. CYC effect on GSH in WB344 and V79	81

INTRODUCTION

Glutathione:

↓
If cells were to elect a "most valuable player" from among their cytoplasmic constituents, glutathione (GSH) must surely win. Aside from being the most prevalent cellular thiol (1), it performs feats beyond the grandest expectations for a simple three amino acid peptide.

Glutathione has been extensively reviewed (1,7,9), and it is not my task to do so again. However, it will be the purpose of this report to investigate some of the mechanisms by which cells produce and maintain their pool of GSH. Toward that end, to follow is a brief outline of the synthesis and metabolism of glutathione and its utility in cellular ecology. (2) ←

Synthesis: Figure 1 represents one of those interminable circle and arrow diagrams dear to the hearts of biochemists; much resembling the "glossy 8 X 10 photos" of Alice's Restaurant fame, it nevertheless takes on a simple elegance on closer examination. Our hero, glutathione, sits prominently in mid stage (actually in mid cytoplasm) but to get there the necessary parts must be hauled into the cell and assembled.

Precursor amino acids cysteine (CYSH), glutamate (GLU) and glycine (GLY) enter the cell by one or more transport systems, depicted in figure 2. Glutamate and glycine's influence upon the rate of GSH synthesis is limited as they

both are found in abundance and can be synthesized by several metabolic pathways. Although the transport of cysteine is more efficient than cystine (2) it is found in low concentration in plasma, and in cell culture media without specific reducing agents cysteine is completely oxidized to cystine (1). The most current review by Deneke *et al.* concluded that in cultured cells cystine uptake is the normal rate-limiting step for GSH synthesis; once inside cystine is rapidly reduced to cysteine (1).

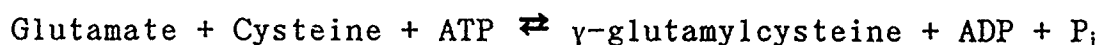
Of the cystine transport systems, X_c^- (Na^+ - independent) is the most specific. Bannai *et al.* report evidence of an exchange mechanism by which intracellular glutamate, generally in abundance, is the currency traded for cystine import (2). The transport activity can be induced by diethyl maleate (DEM) (3), hypoxia (4), sulfobromophthalein (BSP) (5) and elevated pH (6). Several studies have reported that cycloheximide and actinomycin-D blocked the increase in cystine transport, indicating that protein synthesis and/or RNA formation may control X_c^- activity (99, 105). System X_c^- activity is strongly inhibited by excess glutamate in extracellular media, a finding which supports the exchange model (107).

Cells have a few other tricks to get the "makings" inside. The membrane bound enzyme γ -glutamyl transpeptidase (GGT) waves its glycoprotein tentacle in the current like an anemone and captures passing GSH, which it then hydrolyses

to a γ -glutamyl moiety and cysteinylglycine. The later is cycled to produce new GSH, but the enzyme does not stop with simple conservation. Instead it goes fishing in the extracellular stream using the γ -glutamyl group as bait. And the amino acid most likely to "bite" is not surprisingly cystine (7,8). The distribution of GGT and the ability to use extracellular GSH is not universal among cell types; kidney and intestinal mucosal cells have the highest GGT activity (9). Certain hepatocytes isolated from carcinogen treated rats have been shown to utilize extracellular GSH by expressing high levels of GGT (10). This and similar findings have led to the idea that elevated GGT may be used as an early indicator of neoplastic change (11).

Finally, hepatocytes have another option by having the ability to synthesize cysteine from methionine via the cystathionine pathway (8).

From the previous discussion and figure 1 we can see that γ -GCS may obtain substrate by: 1.) transport of CYSH (or cystine), GLU and GLY into the cell directly, 2.) scavenging CYSH from recycled cysteinylglycine and adding GLU obtained courtesy of the γ -glutamyl moiety from GGT or 3.) synthesizing CYSH in the case of hepatocytes. Once the ingredients have been collected the first step in assembly is that catalyzed by γ -glutamylcysteine synthetase (γ -GCS):



In their landmark report Richman and Meister (12) describe the regulation of γ -GCS as nonallosteric inhibition by the endproduct GSH. They found GSH inhibition is competitive with respect to glutamate and that both the sulfhydryl group and the γ -glutamyl moiety were necessary for inhibition. Their calculated apparent K_i value for glutathione of 2.3 mM is within the physiologic range reported for rat liver of 4.5-6.5 mM (9) and would suggest that γ -GCS spends most of its time in a repressed state (no- not Mississippi!). These observations are supported by more recent studies with isolated bacterial γ -GCS which demonstrate the quantitative aspects of GSH inhibition to be virtually the same as rat kidney γ -GCS, although the bacterial enzyme lacks an active site thiol (13).

Other specific γ -GCS inhibitors have been developed. Buthionine sulphoximine (BSO) is commonly used for this purpose. Its action is felt to be specific and does not appear substantially to alter other enzymes involved in the formation or disposal of reactive metabolites (14). It is interesting to note the rate of GSH depletion in various cell types follows their relative GGT activity. In mice, BSO injection depleted liver GSH over a 4-6 hour period. By

comparison kidney, with its much higher GGT content, depleted to 33% of control values within one hour (14).

After γ -GCS has produced γ -glutamyl cysteine, the last step is left to glutathione synthetase (GS):



This reaction proceeds without incident given adequate ATP and a steady supply of γ -glutamyl cysteine for ammunition (8).

Metabolism/utilization: The metabolic and transport functions of GSH are several. From the previous discussion of GGT it is apparent that GSH participates in the transport of various amino acids into the cell via its γ -glutamyl moiety (15). Evidence supports GSH's role in the biosynthesis of prostaglandins and melanin as well as other cellular constituents (90-92).

But the most pressing business for GSH to attend to is the protection of the cell against oxidative challenge and the maintenance of cellular redox status; the literature is inundated with related articles. Glutathione protects against the electrophilic radicals induced by ionizing radiation and chemicals such as hydrogen peroxide, evident by the fact that cells depleted of GSH are damaged more

readily by these agents (15,16). Some metal ions, most notably copper, are rapidly complexed with GSH then "handed off" to metallothionein, a sort of end run play in the cellular superbowl (17). The ability of GSH to prevent some cancers in a dose dependent manner have been linked to its well known free radical scavenger role and some reports suggest that extracellular GSH may detoxify oxidants before they can reach their intracellular targets (18).

The family of glutathione S-transferases detoxify a broad range of electrophilic compounds by catabolically binding them with GSH (19). Made up of a group of related isozymes, the GST(s) are present in most mammalian tissues (19) and many have been genetically sequenced including rat (19,21), mouse (20) and human (22,23). The utility of DNA cloning techniques makes study of GST regulation/expression much easier. It is known that the steady state expression of mRNAs for individual isozymes can vary considerably during liver development (24), dietary changes or even time of day (25). Multiple regulatory elements have been identified for the rat Yp isozyme gene (26) and evidence indicates that gene amplification may be the manner by which GST isozymes are up-regulated in response to a toxic challenge (27). In addition rat liver GST activity can be increased by reduced oxygen species (28) and thiol/disulfide exchange (29). The large knowledge base about how GSH is

used by GST conjugation reactions provides a basis for my study of how GSH is *made* to meet the cell's requirements. It is fair to ask if those stimuli which up regulate GST will also increase γ -GCS, and so I shall.

In conjunction with maintaining cellular redox status there is increasing evidence that the ratio between reduced and oxidized glutathione (GSH/GSSG) may serve as a "trigger signal" for modulating cellular activity (9). The formation of GSH-protein mixed disulfides is strictly correlated to that ratio (30). GSH conjugates have been linked to the expression of several unique "stress" proteins (31,32). A decrease of GSH *per se*, as occurs with BSO treatment, does not induce at least one of these (SH 30) indicating that cellular redox status via reacted or modified GSH mediates that induction (33). If the evidence from bacterial studies showing that stress protein induction may constitute a protective mechanism (34,35) is correct, GSH residues may constitute a "call for the calvary" when the cell is surrounded by xenobiotic indians.

The final loop in the "octopoid" figure 1 demonstrates the reduction of oxidized glutathione via the NADPH-dependent enzyme glutathione reductase. The activity of this system is such that under normal conditions the scales are heavily balanced in favor of GSH in its reduced form (1,9). And since NADPH is a necessary factor (15), both the

pentose phosphate pathway and redox states must be up to speed for cellular GSH pools to persevere.

Cell culture:

Hepatic cell cultures have been advocated as an excellent model for assessing toxic injury (36) and there is little question they have provided much information about *in vivo* response to toxic challenge (37). Kera *et al.* for example found a heterogeneous distribution in the ability of perivenous and periportal hepatocytes to replenish GSH, an *in vitro* result which may explain the greater vulnerability of the perivenous region in intact liver to xenobiotic damage (38). The redox regulation of GSH-protein mixed disulfides discussed before has been examined using hepatocyte culture (30) as has the induction of enzyme systems which determine the metabolic fate of xenobiotics (39). Glutathione S-transferase expression (40,41,42,43), cytochrome P-450 activation (44,45,46), GGT stimulation (40), and neoplastic transformation events (47,74) are representative of the systems which have been successfully modeled in culture.

Their utility notwithstanding, primary hepatocyte cultures are not without liability. In a massive review, Grisham (36) discusses various culture systems and their limitations. He points out that the chief difficulty with primary hepatic culture is the inevitable loss of viability

in isolated hepatocytes with time. Even recent work describing the "long-term" survival of primary cultures when treated with various chemicals only extended their useful life time to about 1.5 months (48,49,50). Primary cultures show marked sensitivity to media composition in their ability to express "normal" *in vivo* enzyme activities (36,42). Finally, serially propagated cells derived from primary cultures often become aneuploid and may be tumorigenic if injected into a susceptible host animal (37).

By serial passage several immortal hepatic cell lines have been developed which morphologically resemble epithelial cells (36,51). Debate has raged about the exact source of these cells, some contending they are biliary epithelial cells, hepatocytic progenitor stem cells, or perhaps both (52). Some reports have drawn parallels between the glycogen storage ability of certain cell lines and preneoplastic glycogen storage foci in the livers of carcinogen treated rats (53). Other lines remain diploid and do not become tumorigenic after prolonged culture and/or frozen storage (54). It is one of these "well behaved" lines, the WB344, that served as a test bed in this project.

WB344: The WB344 cell line was derived from 10 day old Fischer (F344) strain rats. Epithelial cells were selected initially on the basis of morphology - competing

"fibroblast-type" stellate cells were destroyed in culture with a flamed platinum wire, a tedium left to some unfortunate graduate student no doubt! What resulted was a diploid line which grew in monolayer without piling up and had a doubling time of 48 hours. Moreover, even after nine months of continuous culture the cells demonstrated no tumorigenicity upon injection into syngeneic hosts (55).

Table 1 contains several phenotypic characteristics compiled from the literature for hepatocytes, bile duct cells, "oval" cells and WB344. From the patterns observed to date the WB344 seem to express traits somewhere in-between those of mature hepatocytes and oval cells (57). The derivation of oval cells has been controversial. First observed in carcinogen treated livers, the consensus is that they initially arise from a few small cells located near bile ducts in normal liver (56). They mimic the isozyme expression pattern of differentiating hepatocytes during the early proliferative stages of carcinogenesis, an observation which would support their possible role as progenitor cells of hepatocytes. WB344's intermediate phenotype and the reported change of mature hepatocytes in culture toward a "fetal" expression pattern prompts Tsao *et al* (57,58) to speculate that WB344 cells represent a "retrodifferentiated" hepatocyte. Whether they are indeed hepatocyte stem cells which may be induced to differentiate remains to be seen.

The literature on WB344 cells notes that they are growth inhibited by epidermal growth factor (EGF) treatment when in early passage but the effect disappears in late passage, becoming more like the EGF response of mature hepatocytes (58). Under treatment with 5-azacytidine they modified their lactate dehydrogenase isozyme expression toward that of mature hepatocytes (59). WB344 cells did not express GGT under stimulation by retinoic acid as did chemically transformed rat epithelial cells, supporting the contention that they are not pre-neoplastic (60). Metabolic cooperation by gap-junctional intercellular communication has been demonstrated in WB344 by Evans *et al* (61). Finally, WB344 cells showed no mutagenic effects when treated with several polybrominated biphenyls, demonstrating their utility as an *in vitro* toxicity test model (62).

I will not attempt to solve the debate about hepatocyte origins. It is interesting, but not central to the goal of establishing regulatory schemes governing intracellular glutathione. I believe the literature is sufficient to sustain that WB344 cells are stable, diploid and capable of expressing most of the enzyme activities of mature hepatocytes. Much like choosing a friend, one need not be in total agreement on every issue but consensus on the major points is nice. Given that definition, WB344(s) are quite friendly.

The objectives of this project are twofold: a) to characterize a stable cell line as a model for study of cellular redox and GSH metabolism, and b) to use that model to investigate the cellular regulation of the glutathione pool specifically emphasizing its synthesis. Specific questions which will be applied include: how does the cell respond to depletion of GSH; will inhibition of γ GCS affect cellular response; is the maintenance of the GSH pool dependent upon DNA transcription or *de novo* protein synthesis; and what correlation exists between GSH synthesis and GSH utilization? Secondly, the training goal of this project is to gain familiarity with analytical and methodological techniques which apply to toxicological research.

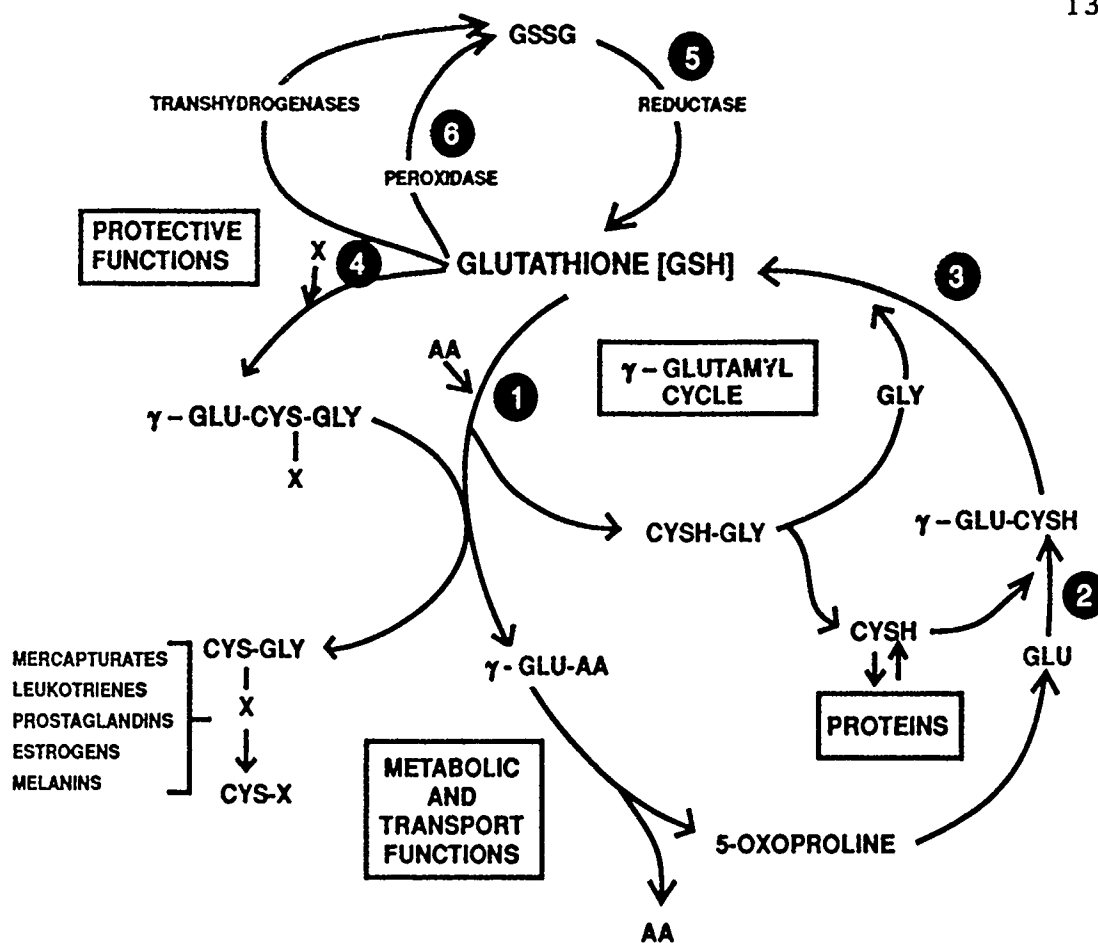


Figure 1. Glutathione biosynthesis and metabolism. *Enzymes:* 1, γ -glutamyl transpeptidase; 2, γ -glutamylcysteine synthetase; 3, glutathione synthetase; 4, glutathione S-transferase; 5, glutathione reductase; 6, glutathione peroxidase. Modified from Meister (7).

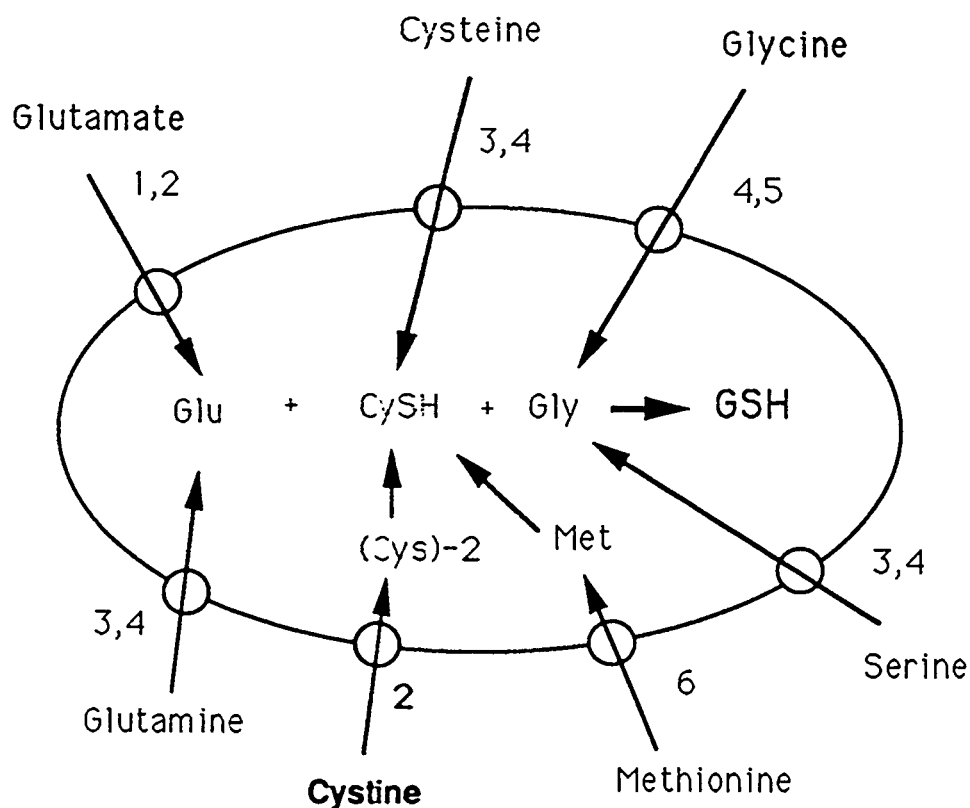


Figure 2. Cellular transport systems for precursor amino acids. *System 1* (X_{10}^-), sodium dependent, specific for anionic amino acids, e.g. glutamate and aspartate; *system 2* (X_c^-), sodium independent, specific for anionic amino acids, cystine and glutamate, not aspartate; *system 3* (ASC), sodium dependent, neutral amino acids with small side chains, e.g., cysteine, serine, glutamine; *system 4* (A), sodium dependent, neutral amino acids with small unbranched side chains, e.g., glycine, serine, cysteine, glutamine; *system 5* (Gly), sodium dependent, specific for glycine and sarcosine; *system 6* (L), sodium independent, specific for neutral amino acids with large branched and apolar side chains, e.g., methionine. Modified from Deneke *et al* (1).

TABLE 1. Phenotypic Profiles of rat parenchymal hepatocytes, biliary duct cells, oval cells and WB344.

	Hepatocytes	Biliary cells	Oval cells	WB344
Albumin	++	0	+	++
AFP	0	0	+	++
Enzymes				
G6P	+	0	0	0
GGT	0	+++	+++	+/-
Isozymes				
Aldolase	B (A) ^a	A	A,B,C	A ₃ C, C
Pyruvate kinase	L (K) ^a	K	K	K
GST [19,24,73]	Ya Yb1 Yc Yk (Yp) ^a	--	--	SEE RESULTS
Ultrastructure				
Desmosomes	+	+	+	+
Mitochondria	Many, large	Few, small	Few, small	Few, small
Free ribosomes	+++	Scanty	+++	+++
Glycogen	+++	0	0	++ ^b

Modified from Tsao *et al* (57) and Sell *et al* (56). Other references noted in brackets.

^a expressed in primary hepatocytes after 4-8 days in culture (41,94)

^b expressed under phenobarbital stimulation (53)

Materials and Methods

Chemicals: All buffer chemicals were obtained from Sigma Chemical Co., St.Louis, MO. Other reagents purchased from Sigma included: DL-Buthionine-(S,R)-Sulfoximine (BSO, no.B-2640), cycloheximide (CYC, no.C-6255), dimethylsulfoxide (DMSO, no.D-5879), maleic acid diethyl ester (DEM, no.M-5887), 1-chloro-2,4-dinitrobenzene (CDNB, no.C-6369), phenobarbital (PB, no.P-1636), sodium selenite (no.S-1382), aphidicolin (no.A-0781), ortho-phenylenediamine (OPD, 1,2-benzenediamine, no.P-9029), glutathione (GSH, no.G-4251) and 5-bromo-2'-deoxyuridine (BrDU, no.B-5002). Actinomycin-D (ACD, #129935) was purchased from Calbiochem, LaJolla, Ca. The fluorophores monobromobimane (MBB) and monochlorobimane (MCB) are available from Molecular Probes, Inc., Eugene, OR.

Cell culture media and reagents ordered from GIBCO Labs, Grand Island, NY, consisted of: Minimum Essential Media (MEM, 78-5069), Dulbecco's phosphate buffered saline (D-PBS, #310-4200AJ), trypsin-EDTA (#610-5405AE) and penicillin-streptomycin (#600-5145AE). Newborn calf (bovine) serum was purchased from Hyclone Labs.Inc., Logan, UT. Polystyrene culture plates and flasks were used throughout the project and are available from several commercial sources such as Corning, Corning, NY and Costar, Cambridge, MA.

Sample protein values were determined with the BCA Protein Assay Reagent (Pierce Chemical Co., Rockford, IL) using bovine serum albumin as a standard.

I will cite sources of procedure-specific materials within each subsection.

Cell culture and harvest: WB344 cells were a gift from Dr.T.Kavanagh, University of Washington, Seattle, WA. The standard media was essential media supplemented both essential and nonessential amino acids, 10% calf serum and 10,000 U/ml penicillin + 10,000 µg/ml streptomycin (hereafter referred to as D-media). Routine WB344 "stock" was maintained on 100 mm plastic culture plates and media changed every 48 hours. Cells were incubated at 37°C in humidified air containing 5% CO₂.

For subculture or harvest, plates were washed with D-PBS and the cells detached by adding trypsin-EDTA then incubating at 37°C for approximately two minutes. Trypsinization was stopped by flooding the cells with either D-media if for subculture or ice cold D-PBS + 5% calf serum if for analysis.

Growth characteristics and DNA measurements: To establish rudimentary growth parameters cells were plated into 30 mm plates containing D-media at cloning density of approximately 200 cells per plate. After 5 days growth the

plates were washed with D-PBS and cell colonies fixed and stained with crystal violet in 20% ethanol. Colonies were counted and plating efficiency data were reported.

For growth curve data, cells plated at colony density into D-media were collected at 24 hour intervals and counted using a Coulter ZM● cell counter. Protein values were analyzed with the Pierce BCA● assay. Data were plotted as cell number vs. protein content.

DNA content and ploidy were checked at intervals throughout the project using flow cytometric analysis performed by Flow Cytometry Services, Pathology Core, University of Washington. The technique used 4'-6-diamidino-2-phenylindole (DAPI) DNA staining (63) standardized against calf thymocytes.

Flow Cytometric Analysis: For all flow cytometric studies cells were trypsinized as described above and gently triturated to separate clumps. One ml of the sample was transferred to a cell culture tube (Falcon, #2054, Becton-Dickenson, Lincoln Park, NJ) and 10 μ l MCB (1mg/ml in 95% ethanol) added to each. Tubes were immediately placed in a 37°C water bath for a 10 minute incubation in the dark after which the reaction is stopped by quickly chilling the samples on ice. Samples were held in the dark on ice pending analysis.

All flow cytometric studies using MCB as the fluorophore were performed on an arc-lamp illuminated flow cytometer (FACS Analyzer; Becton-Dickenson, Mountain View, CA). Excitation of the bimane-GSH complex was at 360-375 nm and fluorescence emission detected at 400-490 nm. Each sample run was standardized by tuning the signal of 9.58 μm Superbright Fluorospheres[®] (Coulter Corp., EPICS Div., Hialeah, FL) to optimum and locating the signal 1 cm left of center on the oscilloscope monitor. Fluorescence intensity and electronic cell volume signals were simultaneously digitalized and stored as compressed binary files on a DEC PDP-11/23 computer (Digital Equipment Corp., Maynard, MA). The data files were subsequently analyzed after the method described by Kavanagh (12,16) using the MULTI2D[®] interactive computer application software (Phoenix Flow Systems, San Diego, CA). The expanded binary files are displayed as cell scattergrams of log volume verses log fluorescence intensity ("cloud pictures" my daughters call them). To remove cell volume effects the axes are rotated clockwise 45[°] and the volume/fluorescence data are collapsed on the fluorescence (x) axis. The resulting histogram of log fluorescence (x-axis) and relative cell number (y-axis) permits user-defined cell population statistical analysis.

Immunohistochemical/cytochemical staining: Subconfluent 100 mm plates of WB344 cells were trypsinized and suspended in

fresh D-media. Twenty-five μ l aliquots containing approximately 1,000 cells were loaded on 12-window Meloy slides. The slides were incubated overnight to allow cells to attach and then stained with fluorescein isothiocyanate (FITC) tagged antibody against rat α -fetoprotein (sheep anti-rat, ShARa/AFP/FITC) and rat albumin (rabbit anti-rat, RARa/ALB/FITC) obtained from Nordic Immunological Laboratories, Capistrano Beach, CA. Staining and fluorescence photography were performed by Pathology Core Services, University of Washington.

To quantify differential staining, flow cytometric analysis was accomplished as follows: Trypsinized subconfluent cells were suspended in ice cold D-PBS + 5% serum and centrifuged for 10 minutes at 50 X G. The supernatant was discarded, the cell pellet resuspended in 400 μ l acetone and the sample split into two tubes (200 μ l each). Twenty μ l of anti-AFP was added to one tube and 20 μ l of anti-ALB to the other (1:10 final antibody dilution). The tubes were incubated at 4⁰C in the dark for 1 hour. Following incubation the cells were washed by flooding the suspensions with 10 ml chilled D-PBS. The tubes were centrifuged again for 10 minutes at 50 X G and the cell pellet resuspended in 1 ml chilled D-PBS. Tubes were held on ice in the dark while transferred to the flow cytometer.

The stained cells were analyzed on the FACS Analyzer

using $\lambda_{ex}=448$ nm and detecting $\lambda_{em}=558$ nm. Data were evaluated as previously described using MULTI2D[®].

For general morphology, WB344 cells were plated on glass slides and photographed using a Nikon Diaphot[®] microscope and tungsten-corrected film (Kodak[®] 160 tungsten). For histochemical staining, cells grown on glass slides were fixed 15 minutes in 10 % buffered formaldehyde and then stained with hematoxylin/eosin (HE) using standard protocols (64).

³H-uridine and ³H-leucine uptake: To determine optimal concentrations of Actinomycin-D (ACD), cells were cultured in 24 well plates at several densities to yield a range of confluency. After 24 hours to allow attachment, the cells were washed with D-PBS and replenished with D-media containing 0.7 μ Ci/ml ³H-uridine and several test concentrations of ACD (0.01, 0.05, 0.1 and 1.0 μ g/ml). After 12 hours the wells were cleared of media and washed three times with D-PBS. Cells were trypsinized by adding 500 μ l trypsin-EDTA and incubated for 2 minutes at 37^oC. Then 500 μ l of Nonidet P 40 (NP-40, Sigma, St. Louis, MO) was added to each well and the plate incubated at room temperature for 10 minutes to lyse the cells. Two ml of 5% trichloroacetic acid (TCA) was added to precipitate proteins and the contents were passed through a nitrocellulose filter under gentle suction. Following a wash with 5 ml D-PBS the

filters were placed in scintillation vials to dry overnight. For analysis, 4 ml scintillation buffer (Aquamix[®], ICN Radiochemicals, Irvine, CA) was added and each vial counted on a liquid scintillation spectrometer (Packard Tri-Carb 3255, Packard Inst. Co., Laguna Hills, CA) for one minute.

In like manner, wells were treated with D-media + ³H-leucine (5 μ Ci/ml) containing 0.1, 0.25, 0.5 and 1.0 μ g/ml cycloheximide (CYC) for 12 hours. Wells were washed and trypsinized as described above and lysed with NP-40. The contents of each well were aspirated and placed in scintillation vials. Scintillation buffer was added (q.s. to 4 ml) and counts read for one minute on the scintillation counter.

Both experiments were run in triplicate and measured against control wells to give a percent incorporation value of the respective radiolabeled chemicals.

HPLC assay for GSH and γ GCS: The number of cells necessary for these procedures required the use of large culture flasks. A minimum of four 150 cm² flasks, or equivalent, per sample proved adequate. Treatment schedules were planned so that cells would just reach confluency at the time of harvest, thereby minimizing cell-cell sharing effects and still maintaining the sample yields required for assay. After trypsinization the samples were centrifuged at

200 X G for 10 minutes (IEC HN-SII centrifuge, IEC, Needham, MA). The cell pellet was suspended in 1 ml ice cold 0.25 M S-TKM buffer (0.25 M sucrose, 80 mM Tris buffer, 5 mM MgCl₂, 0.25 mM KCl, Ph = 7.4). The suspension was held in an ice bath and sonicated by applying three 5 second bursts (20% power setting) from an ultrasonic cell disrupter (Model W-220, Heat Systems - Ultrasonics, Inc., Farmingdale, NY). I must emphasize that *other methods of cell disruption are inadequate* for these purposes. Several months of trying freeze-thaw and detergent lysis yielded extremely variable protein values indicative of incomplete cell breakdown. Following sonication the samples were centrifuged at 10,000 x G in a refrigerated (4⁰C) Beckman microfuge and the supernatant drawn off; aliquots for other assays were quick frozen in liquid nitrogen and stored at -80⁰C. The approach for bimeane-derivitization of biological thiols has been described by Monroe and Eaton (65). As modified by Hamel *et al.* (66), the process is outlined briefly:

Eighty µl of incubation cocktail (120 mM glutamic acid, 200 mM Tris, 0.2 mM EDTA, 150 mM MgCl₂, 1.0 mM AMP, 10 mM ATP, pH = 7.4) was added to a 20 µl aliquot sample. Following a 5 minute pre-incubation at 37⁰C the enzyme reaction was initiated by adding 50 µl of 1 mM cysteine. After mixing, and an additional 10 minute incubation at 37⁰C, the reaction was stopped by adding 50 µl 200 mM sulfosalicylic acid (SSA). The tubes were centrifuged to

remove precipitated proteins and the samples derivatized by adding 200 μ l of 0.2 M N-ethylmorpholine (NEM) in 20 mM KOH. Twenty μ l of 25 mM MBB was added and the samples were inverted and placed in the dark for 30 minutes, after which the derivatized thiols were stabilized by adding 200 μ l of 200 mM SSA. The samples were again centrifuged to remove precipitates and supernatant fractions analyzed on a Shimadzu LC-6A ternary gradient HPLC using an Alltech 15 x 0.5 cm C18 reverse-phase column. Fluorescence was monitored with a Shimadzu Model RF-535 fluorescence detector (λ_{ex} = 375, λ_{em} = 475 nm) at the high sensitivity setting, necessary because of the small quantities contained in the samples. A prepared GSH-bimane standard was co-eluted to identify the GSH-bimane peak. A Shimadzu C-R5A Chromatographic integrator served to integrate peak areas and conversion to GSH equivalents accomplished with a standard curve.

A second 20 μ l sample aliquot was prepared by adding the incubation mixture but immediately stopping any enzyme action by acidifying the mixture with 50 μ l of 200 mM SSA. This served as the baseline GSH sample. However, because of residual glutathione synthetase activity in the samples and the fact that glycine was present despite repeated D-PBS washing during harvest, incubation samples consistently showed more GSH than the "stopped" samples. The difference between the incubation GSH peak and the endogenous GSH peak was added to the γ -glutamylcysteine (γ -GC) peak area units,

reasoning that the discrepancy represented glutathione synthetase present and active during incubation.

ELISA Assay for GST Isozyme: The Enzyme-linked immunosorbant assay (ELISA) protocol used for GST isozyme analysis has been developed by Dr. Zhi-Ying Chen, Dept. of Environmental Health, School of Public Health and Community Medicine, University of Washington. It relies upon primary antibody specificity toward the enzymes of interest and develops a colorimetric endpoint via a peroxidase-linked secondary antibody reaction. Although the concept is straight forward, several pitfalls await those wishing to incorporate this test. Accordingly, I will discuss my methods in detail.

Standardization: Rat liver cytosol, the result of an intense microsome-gathering expedition, was graciously donated by Dr. H. Ramsdell, Dept. of Environmental Health, University of Washington. The cytosol fraction had been collected from normal control animals and stored at -80°C . Primary antibodies (antisera, rabbit-antirat) against GST subunits Ya, Yb1, Yc, Yk and Yp were obtained from Medlabs, Dublin, Ireland. Secondary peroxidase-conjugated antibody (goat-antirabbit) was purchased from the same source.

Serial dilutions of cytosol were made by adding volumes of coating buffer (Na_2CO_3 1.59 g, NaHCO_3 2.93 g, DDH_2O 1000 ml, pH 9.6). The dilutions were prepared in sufficient

volume to allow triplicate wells (200 μ l each) for each GST subunit. Polystyrene microplates (Immulon 1, Dynatech Labs., Inc., Chantilly, VA) were loaded and stored at 4°C overnight. Similarly, each subunit primary antibody and the secondary (conjugate) antibody was serially diluted in PBS-T (NaCl 8.5g, NaH₂PO₄ 0.2g, Na₂HPO₄(7 H₂O) 2.17g, Tween-20 0.5 ml, DDH₂O 1000 ml, pH 7.4). The dilutions of both cytosol standard and antibodies are designed to span the range of possible absorbance values and thereby determine the optimum linear response for a given cytosol-antibody complex. Typically, cytosol dilutions ran from 1:10,000 to 1:100,000, primary antibody dilutions ranged from 1:1000 to 1:10,000 and conjugate dilutions were 1:5000 to 1:50,000.

Following the completion of the assay (description to follow) data were plotted as protein mg/ml (y axis) vs. mean OD (x axis). The resulting plot was examined and the most linear portion selected for curve fitting. This curve, and the related dilution/protein ranges, became the standard curve for each GST subunit. I should note that the cytosol standard dilutions account for the bulk of the variability in linearity, whereas primary and conjugate antibody dilutions mainly affect the intensity of mean OD readings. The object is to obtain an adequate mean OD within the linear range and yet not "swamp" the protein sample with excess antibody. To do the latter only increases cross-reactivity among subunit antibodies; they are not

monospecific! In addition, each lot of antibody must be standardized against whatever standard cytosol one chooses to use. Those limitations in mind, acceptable correlation coefficients ranging from 0.79 to 0.96 were obtained; the regression equations for each subunit curve then allowed transformation of specimen OD values to $\mu\text{g/ml}$ protein equivalents of cytosol standard.

Protocol: Samples previously stored at -80°C were diluted with coating buffer starting with a maximum total protein of $5 \mu\text{g/ml}$ per sample; protein values greater than $5 \mu\text{g/ml}$ will not attach to the test well properly and will wash off. Volumes were calculated to allow for duplicate runs of each sample against each GST subunit. Cytosol standard dilutions were also run each time in duplicate using the linear values obtained as described above.

Generally the cytosol standard dilutions by GST subunit were as follows: Ya - 10K, 25K, 30K; Yb1 - 30K, 40K, 50K; Yc - 10K, 30K, 50K; Yk - 25K, 50K, 100K; Yp - 10K, 30K, 50K.

Test wells are filled with $200 \mu\text{l}$ for each sample following a template which maps the position of standard and specimen wells and their dilutions. Following an overnight incubation at 4°C , excess sample is removed by vigorous shaking and the plate is washed three times by flooding the wells with PBS-T. Two-hundred μl of each primary antibody (1:5000 dilution) is added to wells according to the template, insuring that appropriate subunits are matched

with corresponding sample wells. After a room temperature incubation of 2 hours, the wells are washed three times with PBS-T and 200 μ l of diluted conjugate antibody (1:10,000) is added to each. A 1 hour room temperature incubation follows, after which the wells are washed three times again with PBS-T. The substrate solution (0.1 M citric acid 24.3 ml, 0.2 Na_2HPO_4 25.7 ml, OPD 40 mg, DDH_2O 50 ml) is prepared and 40 μ l H_2O_2 added immediately before use. Following the addition of 200 μ l of substrate to each well, the plate is wrapped in foil and incubated at room temperature for 30 minutes. To stop the reaction 20 μ l of 8 N H_2SO_4 is added and the plate is immediately read on a Molecular Devices \bullet UV₁₁₁ Kinetic Microplate reader at 490 nm.

If the cytosol dilutions were not linear or sample OD values were outside the acceptable range the run was discarded. Data were converted to $\mu\text{g/ml}$ protein equivalents of cytosol standard and graphically displayed as a GST subunit profile. Each GST isozyme was also graphically plotted to show the percent change from untreated control cells included in each experiment. Because of the cross reactivity of some subunit antibodies, the poor linearity of others (most notably the Yp) and the lack of pure antigen standards, data manipulation stopped at this point and no claim for statistical precision will be made. The purpose of these studies was to ascertain gross changes in the pattern of expression among the GST subunits given different

chemical treatments. The assay is *sufficiently* quantitative for that.

GST Activity by CDNB: I used the microplate assay developed in this laboratory (Dr. D. Eaton, University of Washington). Samples stored at -80°C were thawed and diluted with STK-M buffer (dilutions ranged from 1:2 to 1:10 depending on activity). Wells of a polystyrene microplate (Falcon #3915, Becton Dickinson, Lincoln Park, NJ) were filled with 10 μl aliquots of the diluted samples and control blanks were filled with 10 μl DDH_2O . All wells were loaded with 200 μl of substrate solution containing 1 μM each of GSH and CDNB in 0.1 M KPO_4 buffer (pH=6.5). The plate was immediately mixed on the UV_{max}• microplate reader and the kinetic run initiated. Total run time was 2 minutes with data collected every 5 seconds at 340 nm absorbance. All runs were done in at least triplicate and the temperature was held at 30°C . The data, expressed as mOD/min, was converted to nM GST activity/ $\text{min}^{-1}\text{mg protein}^{-1}$ using a standardized activity conversion factor developed by Mr. D. Slone (Eaton Lab., Univ. of Washington).

GSH depletion/repletion: WB344 cells were plated at low density (10,000 cells per 60mm plate) into D-media and allowed to attach overnight. Treatments consisted of depleting cellular GSH with several concentrations of BSO

(1, 10, 100, 250 and 500 μ M in serum-free media) for 2, 4, 6, 8 and 10 hours. Parallel treatments with DEM at 50, 100, and 200 μ M (also in serum-free media) for one and two hours were also performed. Cells were harvested and stained with MCB for flow cytometric analysis as previously described.

From the data, optimum concentrations of DEM = 200 μ l and BSO = 250 μ l were determined. These were used for the repletion studies as follows:

Plates of low density WB344 cells (60mm containing 10,000 cells each) were depleted with 200 μ M DEM or 500 μ M BSO + 200 μ M DEM for a period of two hours. Following the depletion treatment, the plates were washed with D-PBS and replenished with test media containing various inhibitors designed to manipulate a specific phase of GSH synthesis (see results section for specific agents). Control plates were replenished with fresh D-media. Cells were allowed to "recover" from depletion for 2, 4, 6, 8, 10, 12, 24 and 30 hours in the test or control media. At the end of the time series all plates were trypsinized and the cells stained with MCB. Samples were analyzed by flow cytometry as described.

BrDU cell cycle experiment: WB344 cells were plated in D-media on 100 mm plates and were held at heavy confluence for three days. Media was replaced with D-media containing only 0.1% calf serum, thus "serum starving" the confluent culture

for an additional three days. The cells were trypsinized and plated at low density into regular D-media containing 10 μM aphidicholin similar to the method described by Grossman (67). After 24 hours the aphidicholin media was removed, the plates were washed twice with D-PBS and then D-media containing 100 μM bromodeoxyuridine (BrDU) was introduced. Incubation under standard conditions followed, with the added precaution of wrapping the plates in aluminum foil to protect them from light.

Starting 12 hours after the introduction of BrDU, and in four hour increments thereafter, cells were washed, trypsinized and suspended in D-PBS containing 5% serum. The suspensions were centrifuged at 50 X G for 10 minutes and the cell pellet resuspended in D-PBS containing 10% serum and 10% DMSO. The samples were slowly frozen at -20°C and stored at that temperature pending analysis.

Analysis followed the procedure described by Rabinovitch *et al.* (68,69) for two parameter DNA measurement. The thawed cells were pelleted and resuspended in Hoechst 33258 staining solution (0.154 M NaCl, 0.1 M Tris, 0.5 mM MgCl_2 , 0.2% bovine serum albumin, 0.1% Nonidet-P40 and 1.2 $\mu\text{g}/\text{ml}$ Hoechst 33258). Following a 30 minute incubation, 800 μl of the Hoechst stained cells was added to 5 μl ethidium bromide and 25 μl of 500 μM MgCl_2 . Flow analysis was performed using an ICP-22 cytophotometer (Ortho

Diagnostics Systems, Westwood, MA) interfaced to a Dell 386, IBM compatible computer (Dell Computer Corp., Austin, TX).

Data analysis was accomplished with MULTI2D[●]. Briefly, each cell cycle population was outlined and counted. The resulting population statistics allowed calculation and display of cycle-specific cell characteristics and compartment transit times (see results). Cell population profiles were graphically displayed with the isometric option and each cycle compartment label as: a) G1, S, and G2 for first cycle, b) BG1, BS, and BG2 for second cycle and c) BBG1, BBS and BBG2 for third cycle populations, indicating the relative substitution of DNA with BrDU.

Data analysis: The collected mean values of multiple treatments were analyzed by ANOVA using the statistics programs SYSTAT[●] (SYSTAT, Inc., Evanston, IL) and StatView[●] (BrainPower, Inc., Calabasas, CA). If found significant, both the Tukey and the Scheffe-F test for post-hoc comparisons were applied. Only pairwise comparisons which returned a p-value < 0.05 for *both* tests are reported as statistically significant. For pairwise hypothesis testing of two independent samples a Student's t-test was performed using the same programs. Unless noted otherwise, all test for significance are reported at the 95% confidence level.

RESULTS:

Morphology:

In early culture WB344 cells show a moderately large cytoplasm/nuclear ratio (figure 3). Cytoplasmic structure is sparse, limited to some granularity especially concentrated in the perinuclear cytoplasm, especially conspicuous when differentially stained (figure 4). Not unexpectedly, mitotic figures and binucleate cells are common in subconfluent cultures.

Soon after plating, small cell islands form which exhibit some heterogeneity in appearance (figure 5). The central cells are compressed and more polygonally shaped than peripheral cells and tend to stain more intensely acidophilic. Peripheral cells retain the epithelial, almost squamous, look typical of isolated cells.

At confluence the cells are more uniform in appearance (figure 6) although centers of smaller, more densely packed cells are seen and retain the acidophilic differential staining seen in clusters which form early on (figure 7). The cells generally align themselves into "cords" at confluence (figure 8) which sweep around the dense centers. When held at confluence, the central cells become compressed and the nuclei are very dark, almost pyknotic. Mitotic forms were rarely seen in the central areas, suggesting that these are "aging" areas at which dying cells are replaced by the larger "cord area" cells.

Growth characteristics and DNA:

In culture WB344 cells grow in the typical logarithmic-to-plateau curve of most cell culture systems. A doubling time of 28 hours was observed (figure 9). This finding is in the 23-48 hour range reported by Tsao *et al* (57). In exponential-phase growth protein yield was 1.52 mg per million cells (figure 10). Plating efficiency exceeded 90% (duplicate tests, n = 3 plates each).

DNA analysis was performed early in the project and repeated at the midpoint and the end after 80+ passages. No evidence of aneuploid DNA content was found (figure 11).

Albumin/Fetal protein expression:

As seen in figures 12-14, WB344 cells express albumin (ALB), α -fetoprotein (AFP) and vimentin. The ALB and AFP confirm earlier reports (57) and a strong vimentin staining place these cells firmly within the epithelial family.

Acting on an unpublished report from Dr. J. Trosko, Univ. of Mich. (as communicated to Dr. Kavanagh) we treated the cells with 20 mg/ml diethylstilbestrol (DES 99%, Aldrich Chemical Co., Milwaukee, WI) for two weeks attempting to "push" them toward a more mature hepatocyte phenotype. He reported that DES treatment "turned on" albumin expression and repressed AFP, actions typical of fully differentiated hepatocytes (49,50).

Immunostaining photography was equivocal; DES treated cells remained positive for ALB, AFP and vimentin (Figures 12-14 and 15-17). However, flow cytometry revealed DES treated cells to have highly significant increases in albumin expression over untreated cells (log mean fluorescence 51.34 ± 4.6 vs. 49.39 ± 4.1 , $p < 0.001$, $n > 2000$). Also, DES treatment significantly reduced AFP levels (log mean fluorescence 50.15 ± 4.29 vs. 53.74 ± 3.64 , $p < 0.001$, $n > 2000$).

γ -GCS and GST induction/expression:

Phenobarbital: Growth phase cells were treated with 2 mM phenobarbital in D-media for 4 and 6 days. At four days γ -GCS activity was significantly increased over controls: 5.97 ± 0.36 nmoles/min*mg protein⁻¹ vs. 4.98 ± 0.27 for controls, an increase of 19.9%, $p < 0.05$ (table 2). At the same time, GSH values were not substantially different from controls for either four or six day treatments. The level of confluency would seem to be a major influence in the regulation of γ -GCS expression. At day four of treatment cells were just reaching confluence whereas at six days the heavily confluent cells no longer expressed the enzyme at a level different from controls. In both cases the growth suppression effect of phenobarbital is apparent from protein yields of flasks which were initially cultured with

an identical number of cells (table 3). At four days the protein yield per sample averaged 27% less than untreated controls; six day treatment depressed the protein level by almost 33%.

Not surprisingly the GSTs, as measured by activity toward CDNB, were significantly elevated with the four day treatment period (table 3). The 6 day treatment showed significant decrease; this disagrees with other reports of elevated GST expression in confluent WB344 cells (70) but probably reflects the toxicity of this treatment period in WB344 cells.

GST subunit profile obtained from ELISA shows moderate elevations across all subunits for both 4 and 6 day treatment periods except for Ya in the six day sample which remained close to untreated control cell values (figure 18). The pattern itself varies from the "whole rat" cytosol standard (figures 19 and 20) and may reflect differential regulation of GST subunits as has been reported in human lymphocytes by Jones *et al.* (71). In fact, the profile seen in cultured adult rat hepatocytes under phenobarbital stimulation described by Vandenberghe *et al.* (72) is comparable to that of the WB344 cells.

BHA: The antioxidant BHA (200 μ M) was added to D-media and cells were treated for a total of 5 days. As BHA is markedly insoluble in water, DMSO was used as a vehicle to

carry it into solution. Consequently, a DMSO "vehicle control" of 0.4% vol/vol was included in this series. As seen in table 2, BHA sharply increased γ -GCS levels above untreated controls (+72.6%, $p < 0.05$) but caused no increase in GSH. In fact, 200 μ M BHA treatment for 5 days yielded a net decrease in GSH which, however, was not statistically significant. Although 0.4% DMSO did increase the γ -GCS level, it was not statistically significant (+49.1%, $p = 0.095$). BHA's stimulation remained statistically significant after correcting for the vehicle effect. DMSO treatment did not substantially alter GSH values. Both BHA and DMSO depressed protein values equally, reducing them 27% below controls (table 3).

CDNB conjugation by GST(s) was markedly elevated with BHA treatment (+15.3%, $p < 0.001$) but not with DMSO. The later finding is at odds with at least one report of elevated GST activity in freshly isolated rat hepatocytes, however the authors used much higher concentrations of DMSO (up to 2% vol/vol) and found the effect depended largely upon media composition (42). ELISA GST profiles (figure 21) were roughly equivalent for both BHA and DMSO, with the exception of subunits Yb1 and Yk. With BHA, subunit Ya increased by 194% of control values while the DMSO level increased to only 148%. The Yk isozyme was actually depressed by BHA treatment, reaching only 62% of control values while DMSO increased Yk to 138%. The pattern of

isozyme expression, i.e. ranking each according to its relative level within the sample, retained the Yp > Yk > Yc > Ya > Ybl profile observed in control cells (figure 22).

Selenium: Sodium selenite (Na_2SeO_3) was added to D-media to give final concentrations of 10 and 50 μM . Subconfluent flasks of WB344 cells were treated for 24 hours with each concentration. Glutathione levels were not altered by either dose (table 2), but γ -GCS was markedly elevated above controls by the 50 μM treatment (10.61 ± 0.29 nmoles γ -GC produced/min \cdot mg protein $^{-1}$ vs. 6.58 ± 0.88 , $p = 0.011$). A dose response is apparent; although not statistically significant, 10 μM selenium tended to increase γ -GCS (+9.9%, $p = 0.091$); the value is higher still with 50 μM Se. The toxicity of selenium at these concentrations is evident in the depression of protein values with increasing dose (table 3).

GST activity by CDNB was not significantly altered by 10 μM or 50 μM selenium treatments (ANOVA $p = 1.511$). Both concentrations elevated GST profiles with ELISA. All isozyme subunits were elevated slightly above controls with the 10 μM Se treatment level except for Yk, which was depressed to 89% of normal (figure 23). The GST profile reflects the absolute reduction in Yk (figure 24). With 50 μM exposure the isozyme elevations were greater, however these values must be approached with caution. At the higher

dose, the toxicity of Selenium in this cell line alters any physiologic parameter which could be interpreted as a normal cellular response.

Depletion/Repletion studies:

BSO and DEM: BSO was added to D-media at several concentrations and applied to WB344 cells for varying periods of time. GSH levels were followed by flow cytometry using MCB fluorescence. WB344 cells deplete slowly with BSO, reaching values 85% those of control cells when treated with 250 μ M BSO for 8 hours (control log mean fluorescence = 66.8 ± 0.3 vs. 250 μ M BSO at 52.0 ± 0.18 for duplicate samples of $n > 5000$ cells each, t-statistic = 25.024, $p = 0.002$).

DEM time and concentration testing was carried out in the same manner. The most effective concentration was found to be 200 μ M when applied to WB344 cells for 2 hours. This regimen reduced GSH levels by 30%, (control log mean fluorescence = 92.3 ± 0.17 vs. DEM at 70.7 ± 2.7 for duplicate samples of $n > 5000$ cells each, t-statistic = 11.276, $p = 0.008$). All subsequent studies requiring DEM used the 200 μ M for 2 hour protocol.

GSH Overshoot: Figure 25 demonstrates the "overshoot" phenomena observed in WB344 cells following GSH depletion with DEM (200 μ M for 2 hours). Glutathione levels returned

to normal within 5-6 hours and steadily increased to reach a maximum level 120-130% greater than controls by 12 hours. This is very similar to the behavior of C3H 10 T1/2 murine fibroblasts reported by Taylor *et al.* (16), although the response time in the WB344(s) is half that of the fibroblasts (12 hours to peak in WB(s) vs. 24 hours in the murine cell line).

To determine if the overshoot resulted from transcriptional activation of γ -GCS, 0.1 $\mu\text{g/ml}$ actinomycin-D (ACD) was added to the recovery media following DEM depletion. This failed to make an appreciable difference in either the rate or the magnitude of GSH overshoot (figure 26), even though that concentration of ACD is sufficient to inhibit DNA transcription by greater than 75% (75.7 ± 0.69 , $n = 4$) as measured by ^3H -uridine uptake. When ACD was increased to 0.5 $\mu\text{g/ml}$ the repletion curve was comparable to controls although the amount of dead cells increased, indicating this level approached a maximum tolerable dose (data not shown).

Cycloheximide at 1 $\mu\text{g/ml}$ suppressed ^3H -leucine uptake (a measure of intracellular protein synthesis) in WB344 cells by 92.5% (s.d. 2.4, $n = 4$). When added to the recovery media following DEM depletion it increased both the rate and magnitude of GSH recovery over the 30 hour time course (figure 27). This finding was repeated using half the level, or 0.5 $\mu\text{g/ml}$ cycloheximide, with the surprising

observation that the final magnitude of GSH increase was even greater. Furthermore, with both concentrations the overshoot maintained higher glutathione throughout the 30 hour experiment period. This cycloheximide effect was dissected in further studies to be described later.

BSO inhibition: In a series of experiments endogenous γ -GCS activity was destroyed by adding 250 μ M BSO in the treatment media in addition to 200 μ M DEM -- direct depletion by DEM was included to improve resolution of the time course curves following GSH recovery. With this treatment regimen, GSH levels fell to 70% of controls and gradually returned to normal levels in 10 hours (figure 28).

Two possible explanations could account for the recovery: either 250 μ M BSO was insufficient to inactivate all of the original γ -GCS leaving some residual to restore GSH pools or γ -GCS was made *de novo* to supplant the intoxicated original enzyme. The first possibility is unlikely as the 250 μ M BSO level far exceeds any reported intracellular or tissue γ -GCS concentration (14,62,66). Never-the-less, a "fresh" vs. "used" BSO trial was performed by treating cells with 250 μ M BSO for 12 hours, at which time the media was removed and flooded onto untreated cultures. Over the course of another 12 hours the used BSO was as capable of depleting GSH as new BSO media. Both reached significant depletions at 8 hours measured against

controls, log mean MCB fluorescence treated (used BSO) = 37.68 ± 8.12 , $n = 5687$ vs. control (untreated) 43.69 ± 9.41 , $n = 7969$, $p < 0.001$).

If BSO is, in fact, an irreversible γ -GCS inhibitor, either transcriptional activation and translational control of *de novo* γ -GCS synthesis could explain the recovery. Both schemes were investigated by adding first $0.1 \mu\text{g/ml}$, then $0.5 \mu\text{g/ml}$ ACD. Neither concentration stopped the gradual return to normal values of GSH (figure 29). With the $0.5 \mu\text{g/ml}$ ACD, GSH values at 24-30 hours post-treatment actually increased over control values, demonstrating a small overshoot such as is seen in the DEM-direct depletion experiments.

Cycloheximide at $0.5 \mu\text{g/ml}$ and $1 \mu\text{g/ml}$ also failed to prevent the rise in GSH levels (figure 30). Both concentrations in fact accelerated GSH recovery and produced overshoot GSH quantities.

The continued GSH repletion in the face of inhibitor concentrations which should overwhelmingly prohibit new γ -GCS synthesis is perplexing. To determine whether BSO itself would affect the repletion curve it was added to the recovery media at $500 \mu\text{M}$. As seen in figure 31, the depleted GSH values are sustained, indicating continued inhibition of new γ -GCS which may be synthesized during the recovery period. By adding cycloheximide ($1 \mu\text{g/ml}$) to the $500 \mu\text{M}$ BSO recovery media higher GSH values are obtained but

levels persist at sub-control values (figure 32). Whatever the possible mechanisms by which cycloheximide elevates cellular GSH, they likely do not include significantly reversing BSO inhibition of γ -GCS. Nor does it appear that CYC activates GGT to import serum γ -glutamylcysteine moieties, thus bypassing γ GCS altogether. With GGT specifically inhibited by 50 μ M acivicin (ACV), CYC still significantly elevated GSH over untreated control cells: log mean MCB fluorescence in controls = 39.72 ± 0.30 , ACV = 40.64 ± 0.57 , CYC = 42.24 ± 1.10 and CYC+ACV = 42.3 ± 1.37 ; ANOVA sig. at $p=0.002$; ACV vs. controls N.S., CYC+ACV sig. at $p=0.007$ (figure 33).

Cycloheximide: Cycloheximide's behavior in the previous experiments was unexpected. To examine its ability to affect GSH levels with time, subconfluent WB344 cultures were plated with D-media containing 1 μ g/ml cycloheximide. GSH levels were followed over 30 hours by MCB fluorescence and flow cytometric methods described previously. Figure 34 demonstrates the abrupt rise in intracellular GSH; values rise to over 120% in only two hours. Moreover, elevated levels were maintained throughout 30 hours and cell death was minimal.

The increase in glutathione was also measured by HPLC following a 15 hour treatment with 0.5 μ g/ml CYC. GSH levels increased to 225.9% of controls (sig. at $p < 0.001$).

The γ -GCS activity did not change (2.97 ± 0.31 nmoles/min \cdot mg protein⁻¹ vs. 3.06 ± 0.36 for controls, not sig., $n = 2$ samples of four 150 cm² flasks). Cycloheximide treatment did not alter GST-CDNB activity, 20.13 ± 0.42 nmoles/min \cdot mg protein⁻¹ vs. 19.21 ± 0.73 , not sig., $n = 4$.

Perhaps CYC affected the availability of substrate amino acids within the cell, particularly cystine-cysteine. This aspect was examined by flooding subconfluent WB344 cells with a "cystine-free" (CF) media consisting of D-PBS + dextrose (1mg/ml). Duplicate samples were carried for three hours with and without 1 μ g/ml CYC. Controls in D-media were run as well. Table 4 summarizes the data. Cycloheximide significantly increased GSH levels in the presence of normal D-media. Cells treated with amino acid free media did not differ from control cells in GSH content. Cycloheximide failed to increase GSH in the CF treated cells.

The CF media experiment was repeated in chinese hamster V79 cells to see if the effect is idiosyncratic. It is not - V79 cells respond to CYC in the same fashion as WB344(s) if provided with media containing cystine. However, in CF media without CYC the V79(s) demonstrated higher GSH values than controls (table 4); treatment with CYC did not increase GSH further.

BrDU cell cycle kinetics: WB344 cells enter into cell cycling following release very quickly. At 12 hours prominent G1, G2 and BG1 (second cycle G1) are observed (figure 35). When corrected for cell divisions, i.e. second cell cycle count divided by 2, third by 4 and etc., over one quarter (24.78%) of the original cells had reached BG1. Cycloheximide treatment (CYC-TX) at 1.0 $\mu\text{g/ml}$ produced an amazing change in the cycle profile (figure 36). Fully 91.6% of the original cell population had raced through the first cell cycle and accumulated in the BG1 compartment.

By twenty hours after release 30.26% of the original cell population had reached BG2 of the second cycle (figure 37). Only 15.23% remained in BG1, contrasted to 95.5% in CYC-TX cells (figure 38). The disparity is not due to cell death. Small, fragmented or unstained nuclei were not observed in significant numbers.

Untreated WB344(s) had entered the third cell cycle by 28 hours following release, seen in figure 39 as the leftmost peak BBG1. This represents 22.08% of the originals. Cycloheximide treatment resulted in arrest within BG1 at this (and every other!) time point, with 91.4% remaining in that compartment (figure 40).

Progression in untreated cells continued throughout the remaining time points (figures 41-44); at 36 hours WB344 BBG1 = 36.2%, BBS = 11.95% vs. zero for CYC-TX. At the

final time point, 48 hours, 8.51% of the WB344(s) had achieved BBG2; CYC-TX still sat in BG1 with 91.1%.



Figure 3. WB344, subconfluent, no stain, (200 X). Large cytoplasm to nuclear ratio and typical epithelial morphology are apparent. Cells in this photo have been in culture 24 hours.

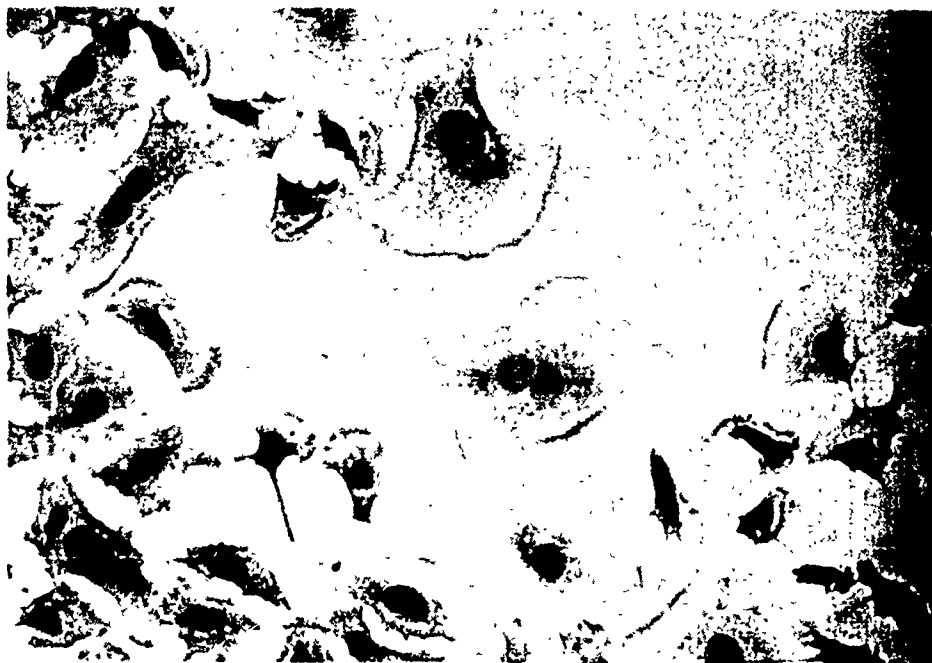


Figure 4. WB344, subconfluent, H&E, (400 X). Perinuclear granularity is demonstrated by differential staining. Other cytoplasmic structure is sparse. Binucleate nuclei (arrow) are common in early culture. Isolated cells develop an almost squamous epithelial morphology.



Figure 5. WB344, cell islands, H&E, (200 X). Cell island colonies form quickly after low density plating (arrow). Heterogeneous morphology is usual; central cells are compressed, some peripheral cells demonstrate a spindle shaped nucleus.

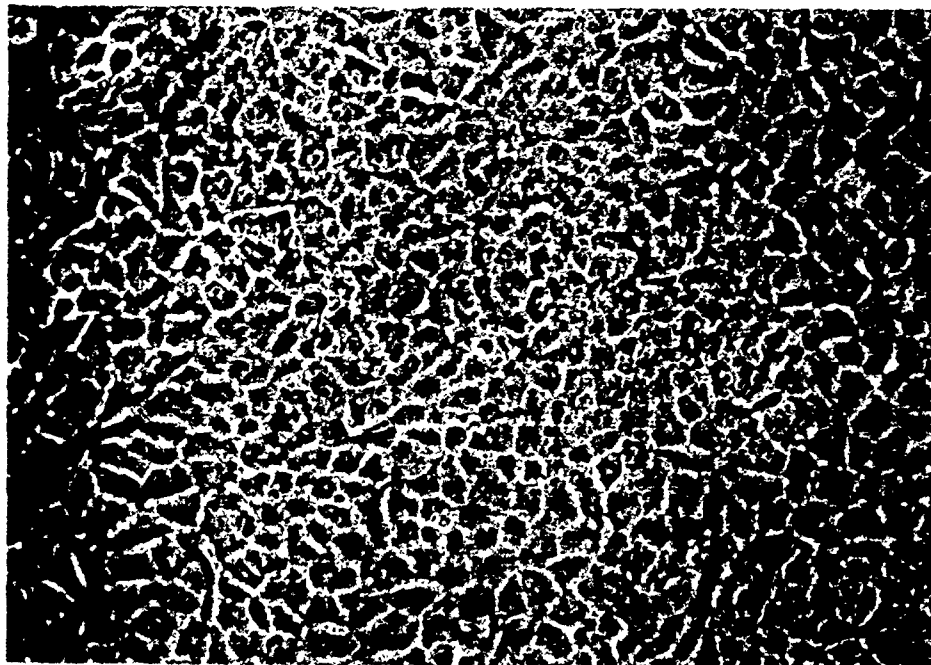


Figure 6. WB344, early confluence, no stain, (200 X).
At early confluence, cells take on a uniform polygonal morphology. Fewer mitotic figures are seen than in subconfluence. These cells have just reached confluence.

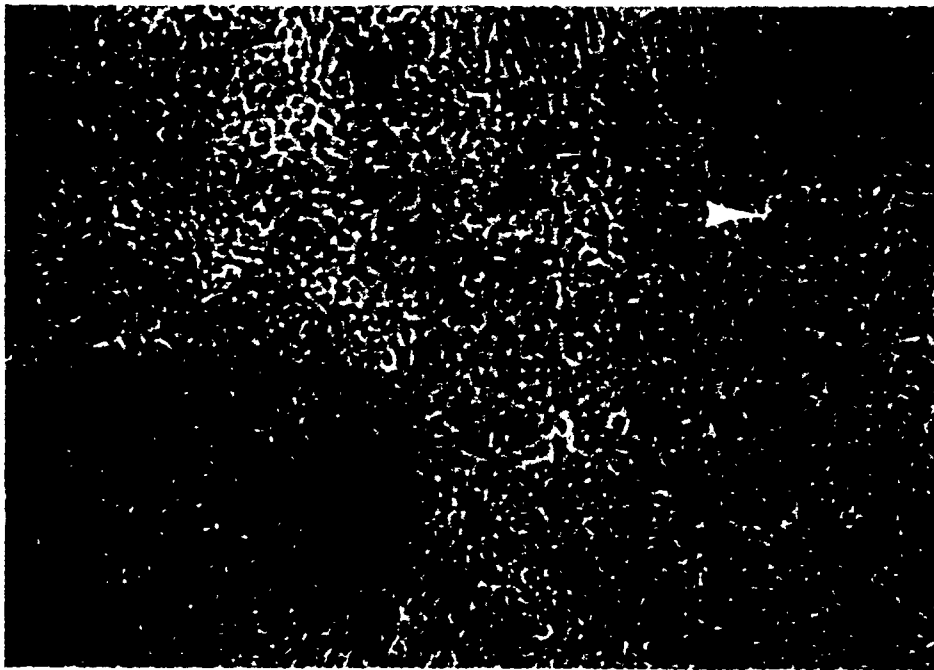


Figure 7. WB344, confluence, H&E, (100 X). Stained culture held at confluence 24 hours. Note acidophilic centers (arrow) of compressed cells.



Figure 8. WB344, confluence, H&E, (400 X). Cells align into cords beginning in early confluence (arrows).

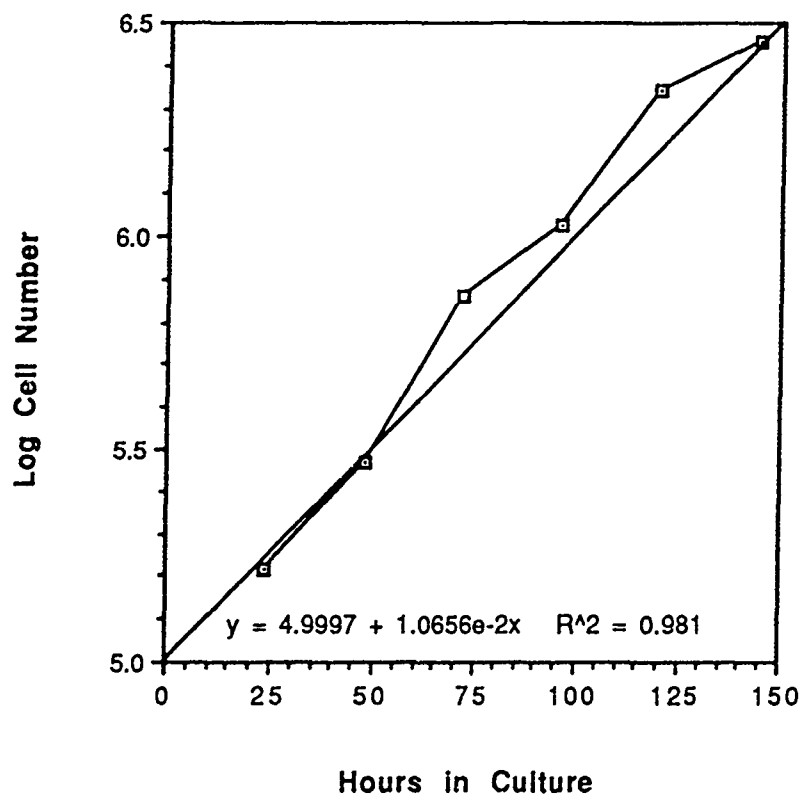


Figure 9. Log cell number vs. time. Cells were plated at colony density as described in methods. Each point represents the mean of triplicate counts. S.D. ranged from 0.9% to 2.5% of mean value.

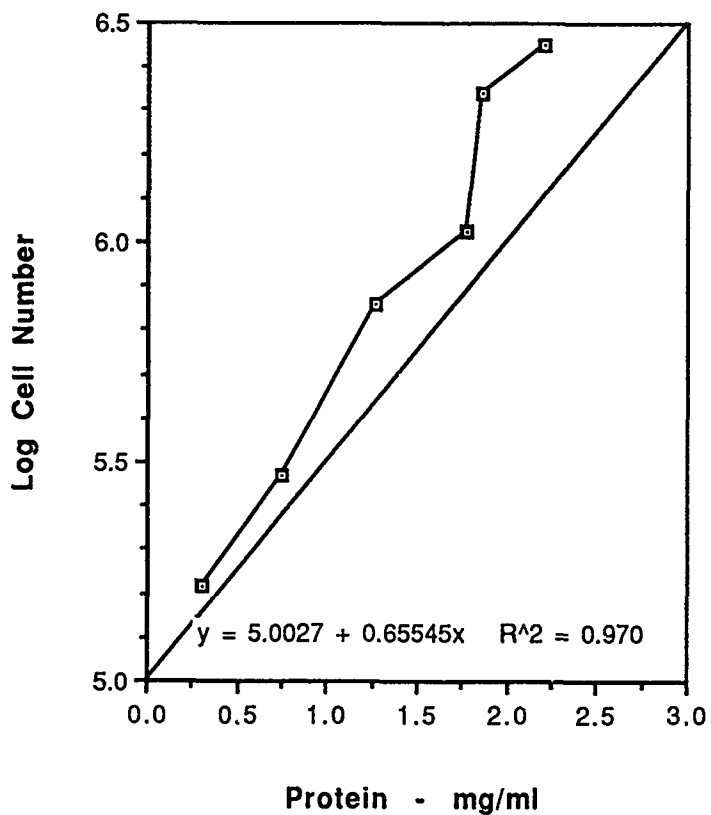


Figure 10. Log cell number vs. protein. Cells were plated at colony density as described in methods. Each sample run in triplicate. Protein values are weighted mean values returned from the Pierce BCA assay as described in methods sections.

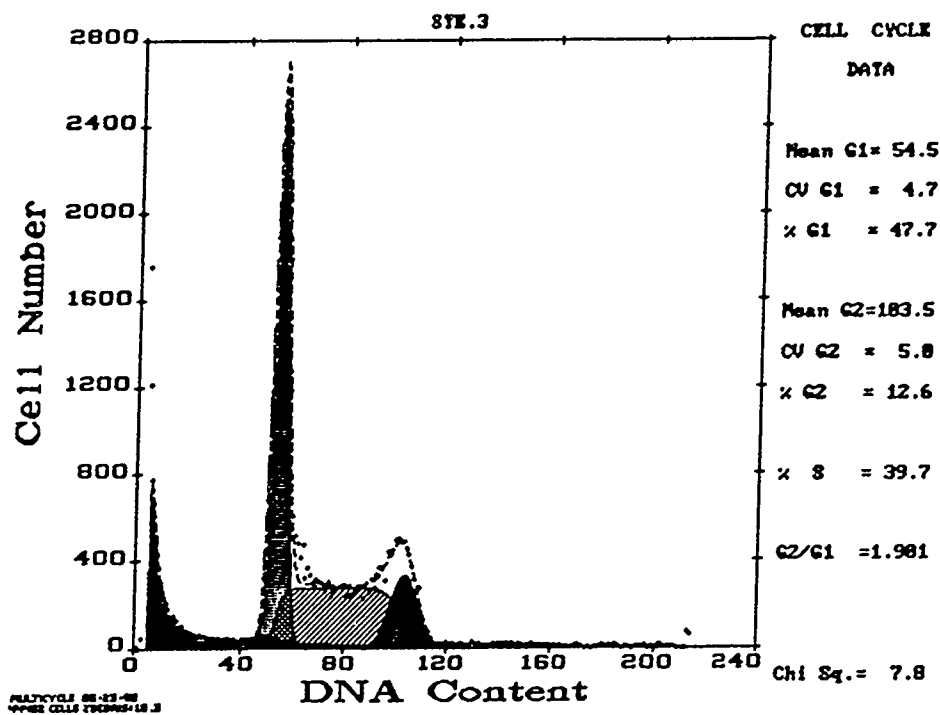


Figure 11. DAPI DNA analysis by one parameter flow analysis. Profile represents DNA profile after 80+ passages. Cells are sampled in the exponential growth phase and show no aneuploid peaks in this profile. High S-phase is typical of fast growth. This profile is identical to others taken at the beginning and mid-point of the project.

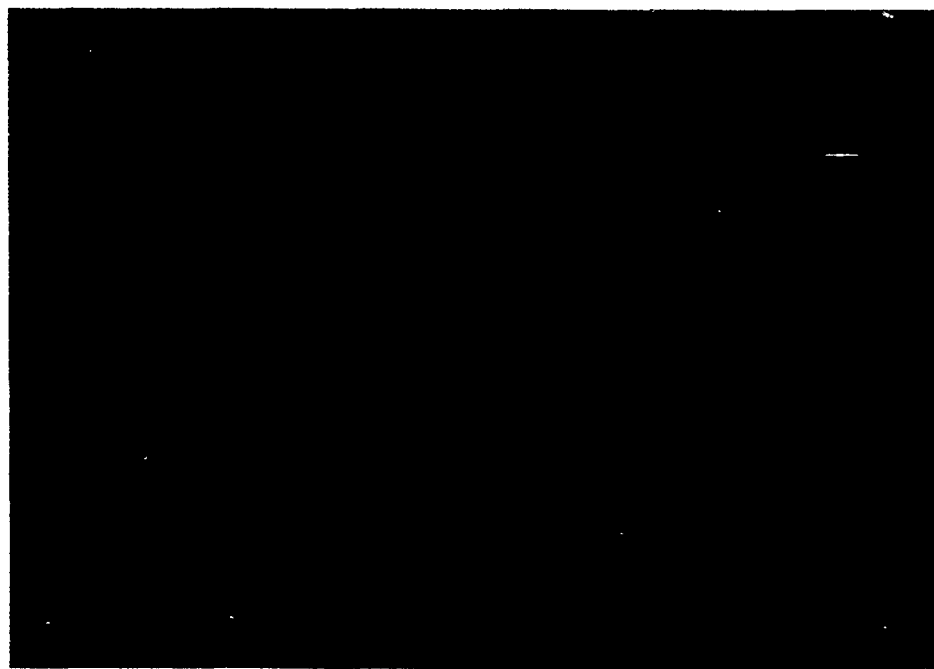


Figure 12. Immunostaining - Albumin, WB344, (600X). WB344 cells express albumin uniformly throughout the cytoplasm.

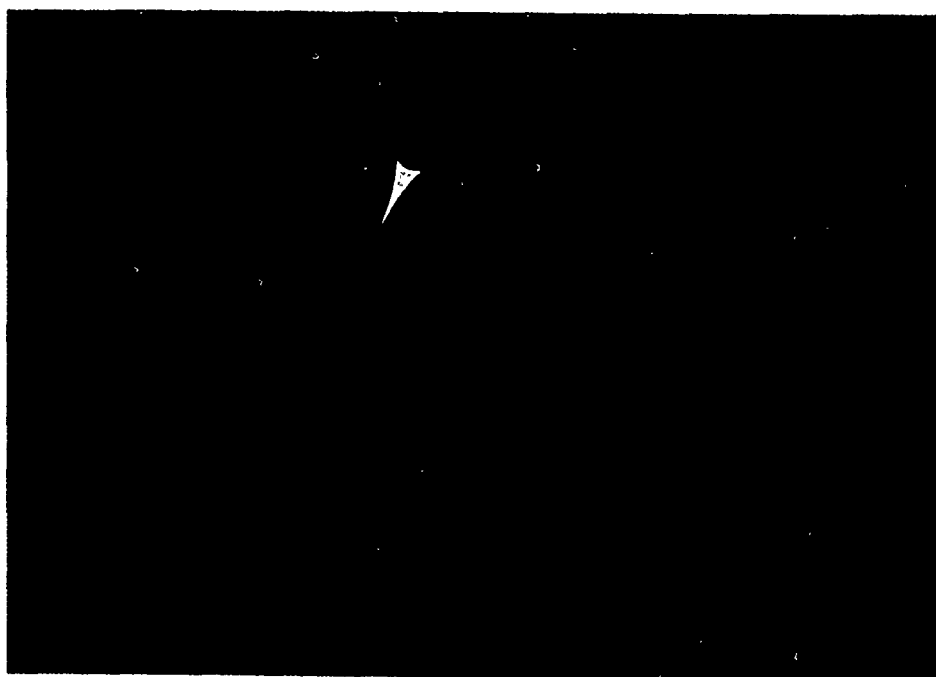


Figure 13. Immunostaining - AFP, WB344, (600X). Alpha fetoprotein is distributed in the perinuclear cytoplasm (arrow).

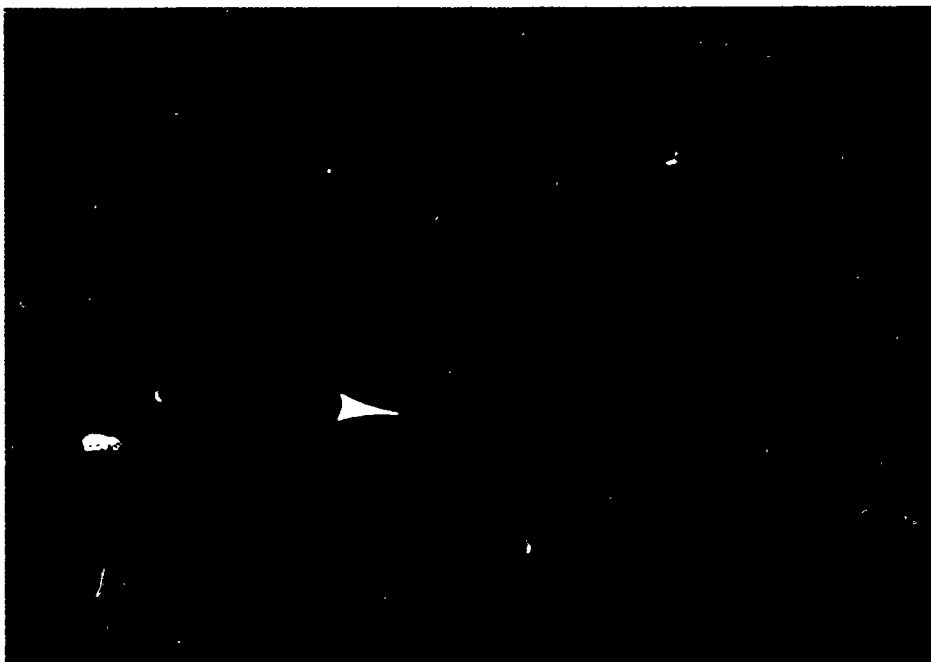


Figure 14. Immunostaining - Vimentin, WB344, (600X). Cellular matrix can be seen along the peripheral cytoplasmic membrane (arrow). This expression is typical of epithelial-type cells.



Figure 15. Immunostaining - Albumin, DES treated WB344, (600X). DES at 20 $\mu\text{g}/\text{ml}$ for 14 + days did not alter albumin distribution. For quantitative comparison see results section.

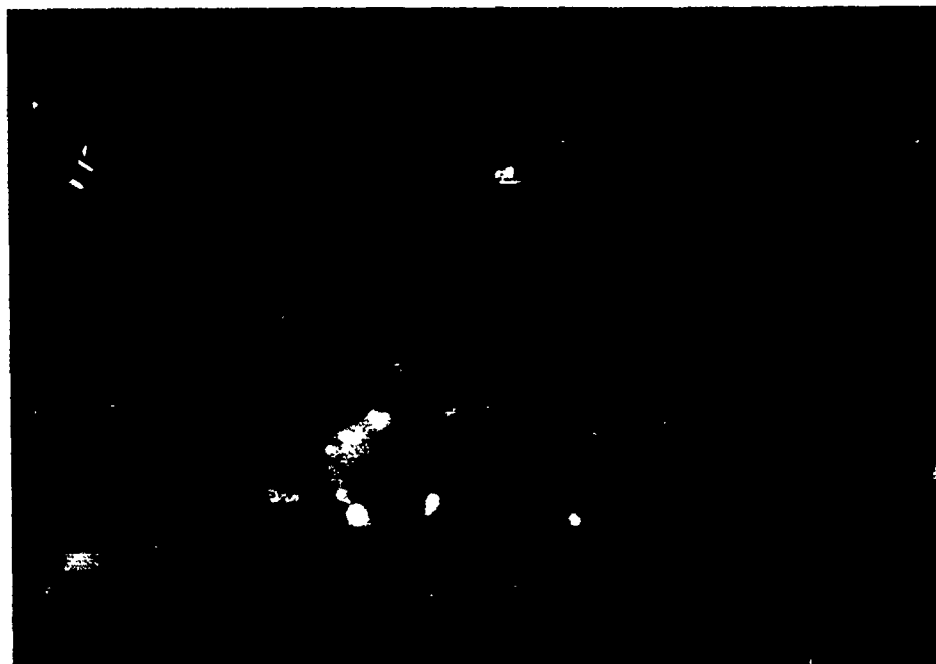


Figure 16. Immunostaining - AFP, DES treated WB344. (600X). DES at 20 $\mu\text{g}/\text{ml}$ for 14 + days did not visibly alter alpha-fetoprotein. For quantitative comparison see results section.

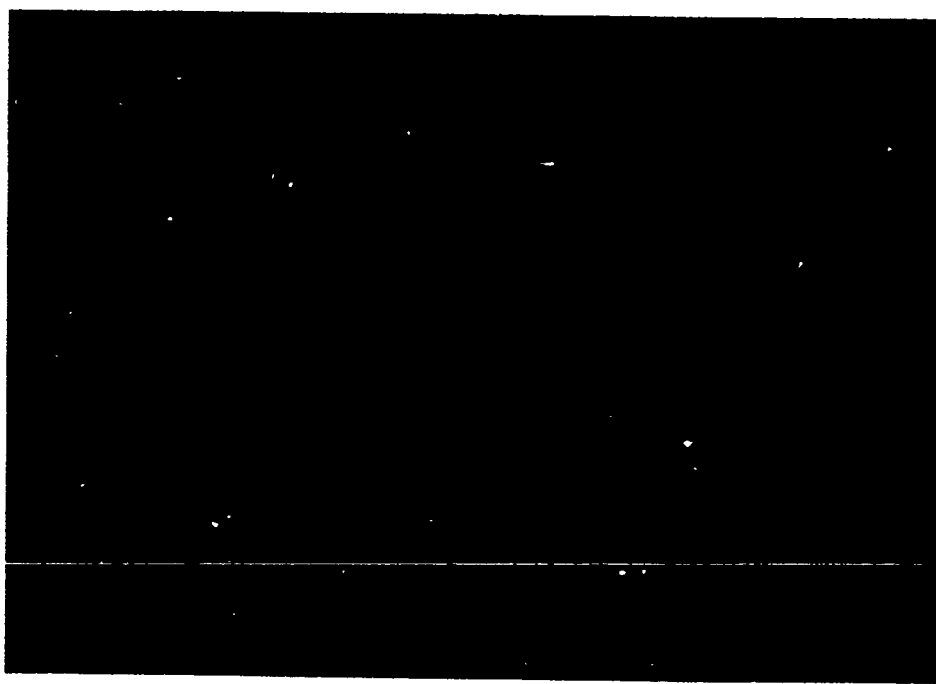


Figure 17. Immunostaining - Vimentin, DES treated WB344, (600X). DES at 20 $\mu\text{g}/\text{ml}$ for 14 + days did not visibly alter the distribution of filaments.

TABLE 2. Induction of γ -GCS in WB344 Cells

Cell Treatment	GSH nmoles/mg protein	γ -GCS [†] nmoles per/min [•] mg protein ⁻¹
Phenobarbital -- 2mM for 4 days	11.69±0.95	5.97±0.36 (+19.9%)*
WB controls	12.43±0.70	4.98±0.27
-- 2mM for 6 days	27.00±1.20	4.1±0.14
WB controls	27.30±1.03	3.8±0.08
BHA -- 200 μ M for 5 days	19.70±3.06	3.02±0.41 (+72.6%)*
DMSO -- 0.4% for 5 days vehicle control	20.68±2.06	2.61±0.26
WB controls	22.97±0.04	1.75±0.10
Sodium Selenite -- 10 μ M for 24 hrs.	24.20±0.05	7.24±0.26
-- 50 μ M for 24 hrs.	30.86±2.53	10.62±2.29 (+61.1%)*
WB controls	28.37±0.81	6.59±0.88

* sig. different from control at $p < 0.05$

[†]represents γ -GCS activity as measured by γ -GC formation
All means and standard errors represent pooled samples from
four or more 150 cm² flasks. All samples were run in
duplicate with controls. Numbers in parenthesis represent
percent change from control values.

TABLE 3. Induction of GST[†] in WB344 Cells

Cell Treatment	Protein mg per ml	GST nmoles per/min*mg protein ⁻¹
Phenobarbital -- 2mM for 4 days	5.66±0.72 (-27.8%)*	18.91±1.34 (+29.5%)*
WB control	7.84±0.45	14.61±0.60
-- 2mM for 6 days	10.63±0.3 (-32.7%)*	47.535±2.06 (-14.3)*
WB control	15.8±0.80	55.47±0.56
BHA -- 200 µM for 5 days	10.84±1.24	21.192±0.22 (+15.3%)*
DMSO -- 0.4% for 5 days	10.48±1.05	19.065±0.21
WB controls	14.4±0.04	18.38±0.94
Sodium Selenite -- 10 µM for 24 hrs.	7.40±0.08 (-13.0%)*	24.479±2.24
-- 50 µM for 24 hrs.	4.04±0.22 (-52.5%)	26.41±0.98
WB controls	8.51±0.89	27.75±0.36

* sig. different from control at p<0.05
[†]represents GST activity as measured by CDNB conjugation
 All means and standard errors represent pooled samples
 from four or more 150 cm² flasks. All samples were run
 in duplicate with controls. Numbers in parenthesis
 represent percent change from control values.

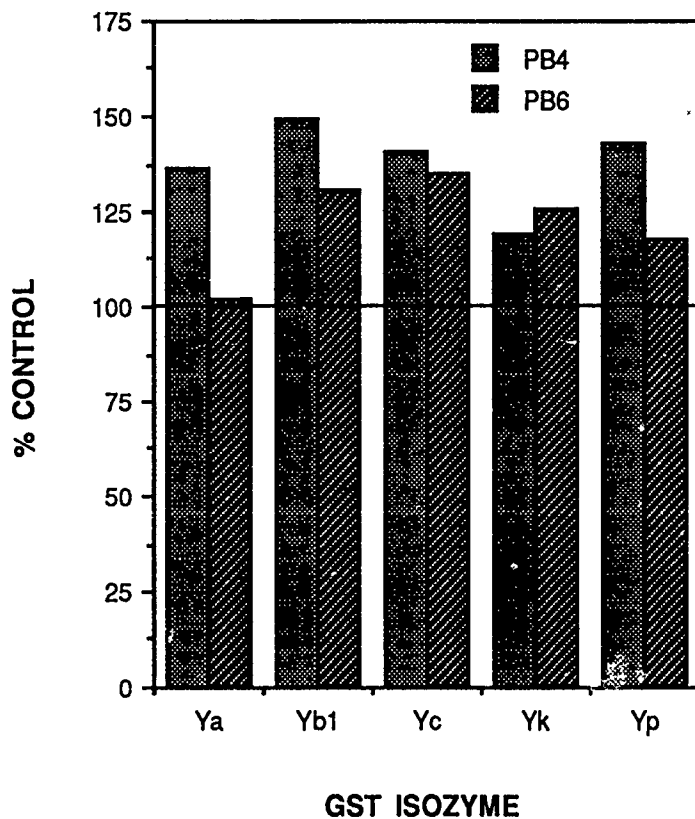
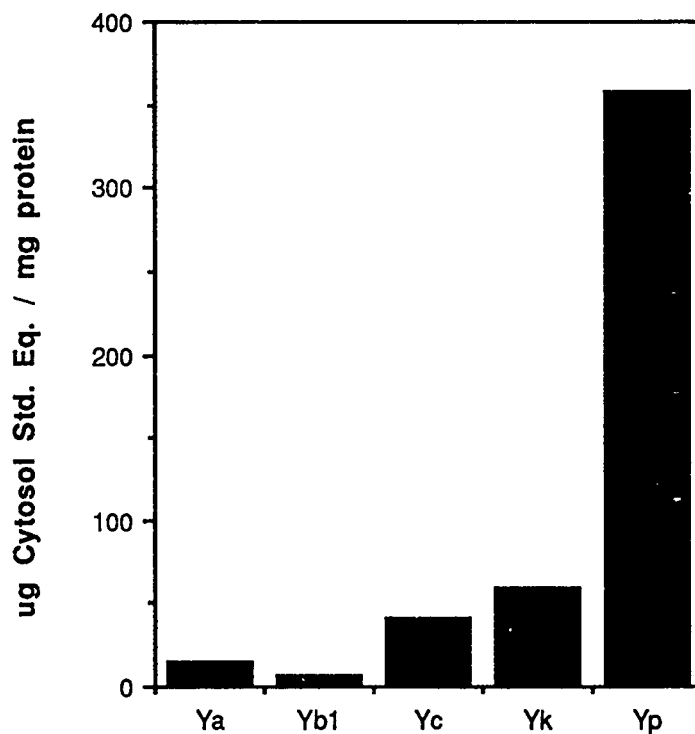
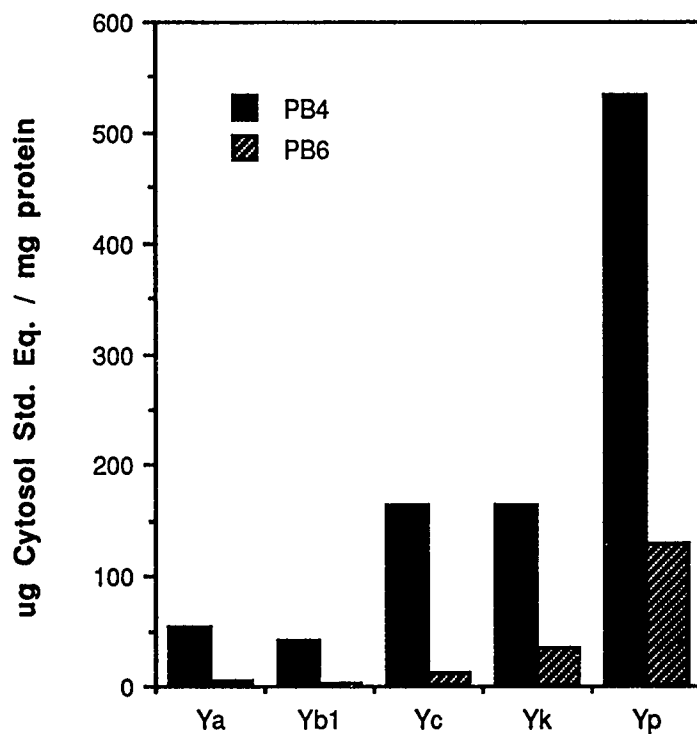


Figure 18. Phenobarbital effect on GST isozymes. Cells were treated with 2 mM phenobarbital for 4 and 6 days. GST isozymes measured by ELISA as described in methods section. Each sample was the sum of at least four 150 cm² flasks. ELISA samples were run in duplicate against untreated controls. Treated samples are expressed as percent of controls.



GST ISOZYME

Figure 19. GST profile of cytosol standard. The combined cytosol of several normal rat livers served as the standard. Values for normal WB344 cells, and subsequent experiments, are expressed as μg cytosol standard equivalents per mg protein of sample.



GST ISOZYME

Figure 20. GST profile of PB treated WB344. The GST profile with four day, 2 mM phenobarbital treatment varies slightly from cytosol standard expression patterns (see fig 19).

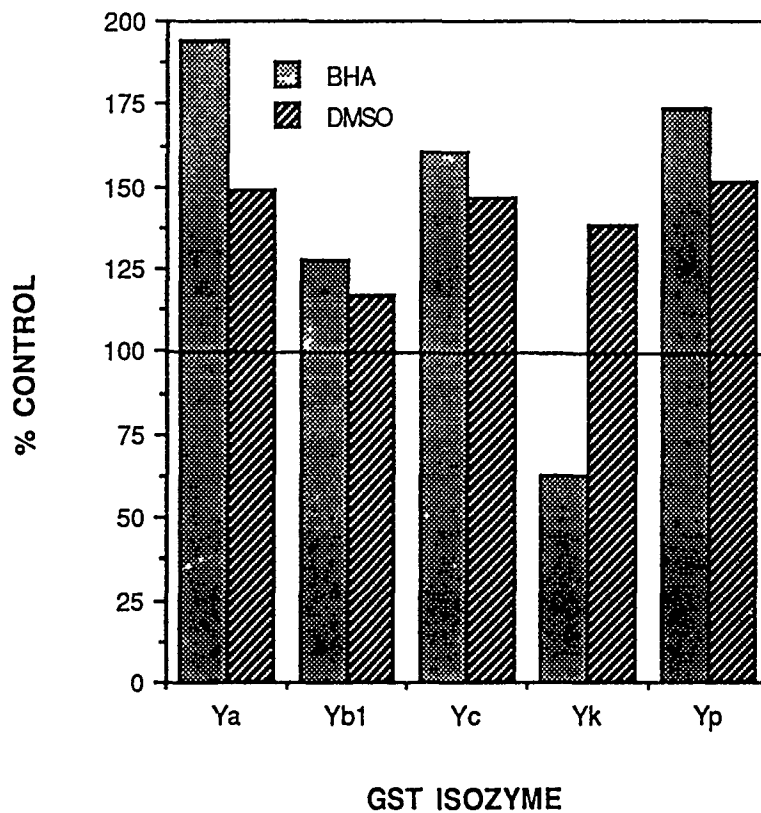
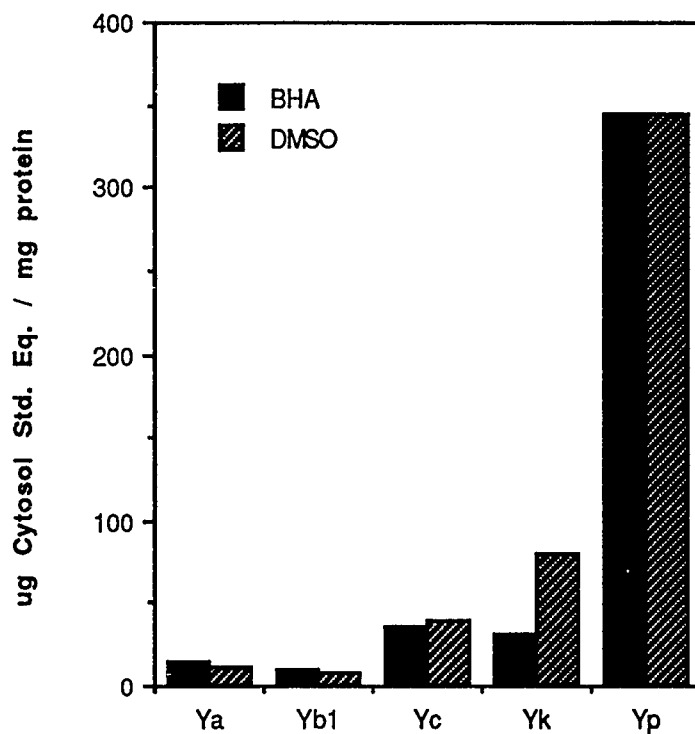


Figure 21. BHA effect on GST isozymes. Cells were treated with 200 μ M BHA for 5 days. DMSO 0.4% vehicle controls were included. Values express the percent of untreated control WB344 cells.



GST ISOZYME

Figure 22. GST isozyme profile with BHA treatment. Cells were treated with 200 μ M BHA for 5 days. DMSO 0.4% vehicle controls were included. Compare pattern with figure 19, cytosol standard.

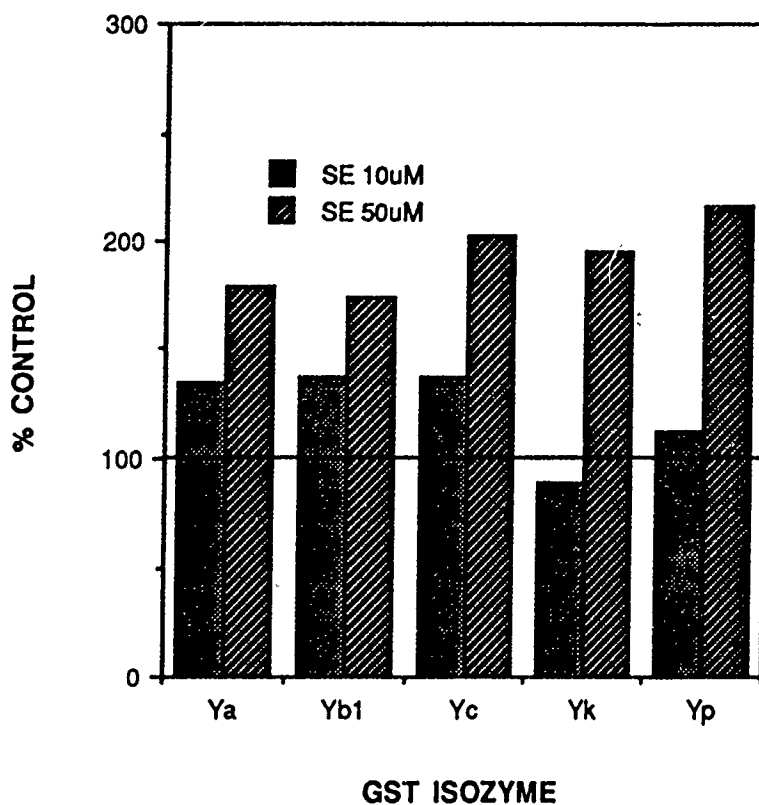


Figure 23. Selenium effect on GST isozymes. Cells were treated with 10 μ M and 50 μ M sodium selenite for 24 hours. The higher concentration approached the maximum tolerated dose in this cell line.

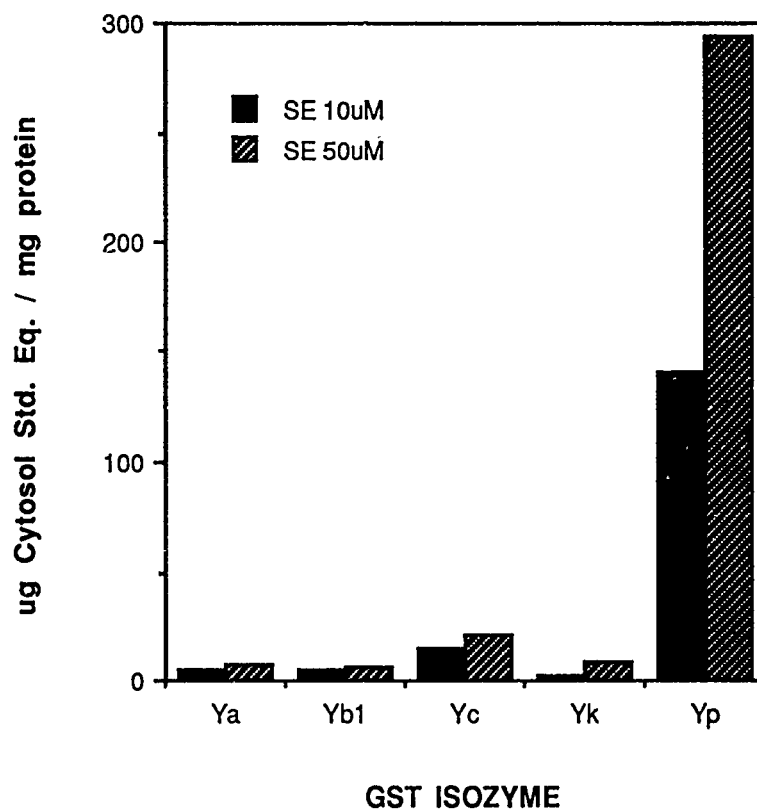


Figure 24. GST isozyme profile with selenium treatment. Selenium treatment reduced the expression of Yk relative to cytosol standard, see fig. 19.

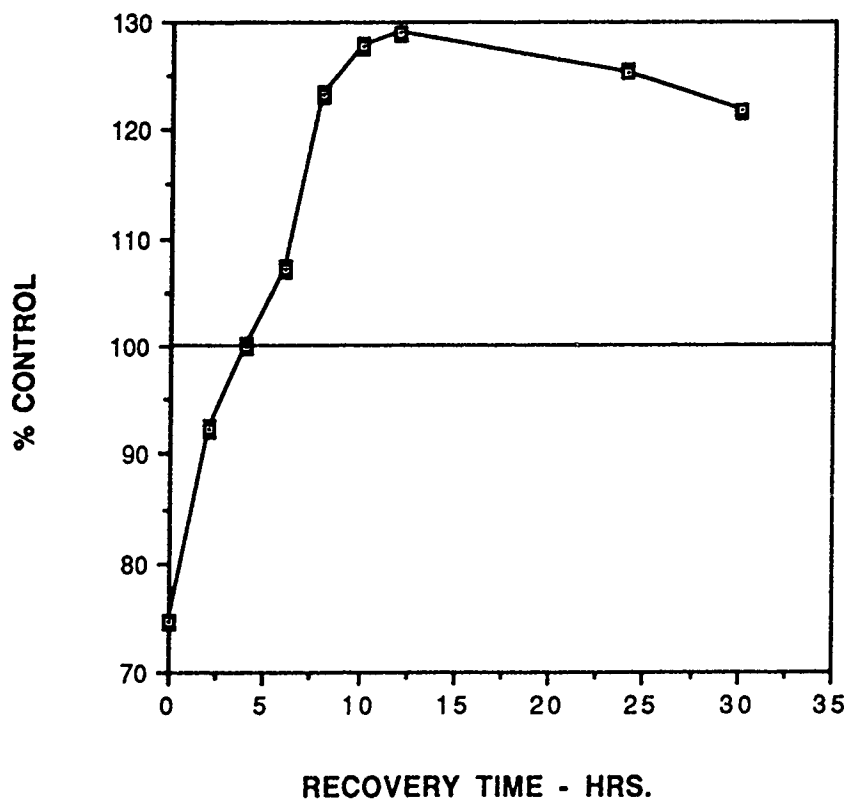


Figure 25. GSH overshoot following DEM depletion. Subconfluent plates of WB344 cells were depleted with 200 μ M DEM for two hours. Recovery in D-media was followed by flow cytometry. Each point is the mean of three separate experiments run against untreated control cells. S.E.M. are plotted but are too small to be immediately visible (S.E.M. = 0.005 to 0.01).

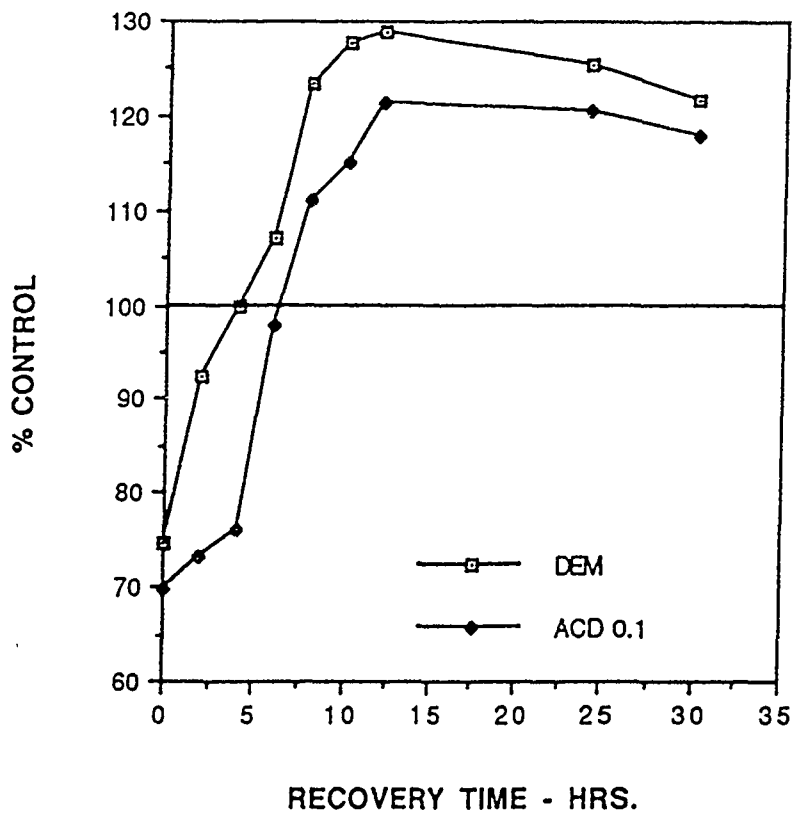


Figure 26. ACD effect on GSH overshoot. Actinomycin D, 0.1 $\mu\text{g/ml}$, did not prevent the overshoot of GSH in WB344 cells following DEM depletion. ACD values are the mean of duplicate samples, $n > 5000$ cells each, S.E.M. = 0.05 to 0.07.

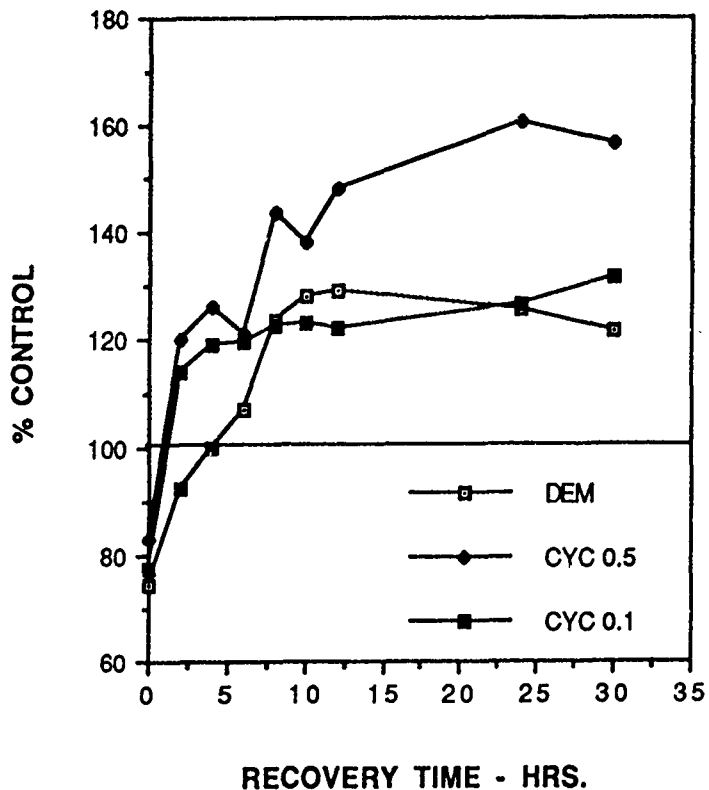


Figure 27. Cycloheximide's effect on GSH overshoot. Cycloheximide at 0.5 $\mu\text{g}/\text{ml}$ and 0.1 $\mu\text{g}/\text{ml}$ did not prevent the overshoot of GSH in WB344 cells following DEM depletion. CYC values represent means of duplicate samples drawn from parallel plates ($n > 3500$ cells per sample, S.E.M. = 0.001 to 0.01).

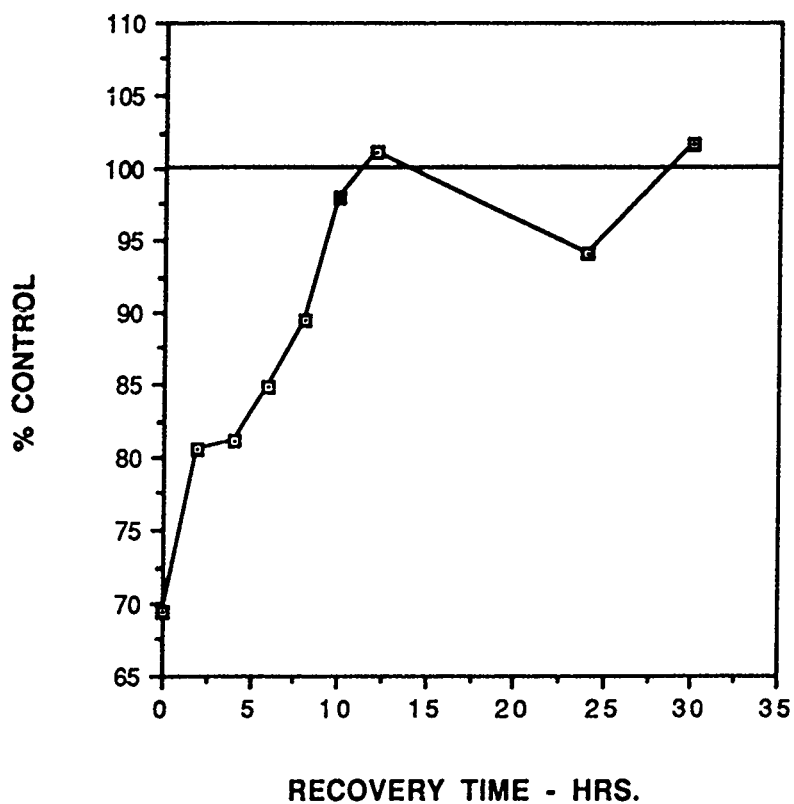


Figure 28. GSH recovery following BSO treatment. Cells were treated with 200 μM DEM and 250 μM BSO for two hours. Recovery in D-Media was followed by flow cytometry. Each point represents the mean of three separate experiments (S.E.M = 0.003 to 0.1).

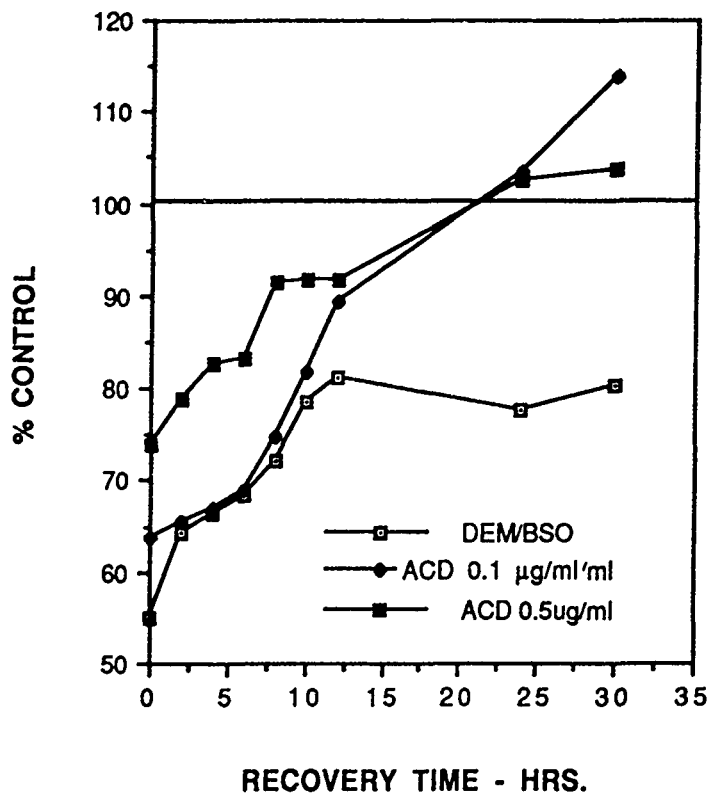


Figure 29. Actinomycin D effect on GSH recovery following BSO treatment. Cells were treated with 200 μ M DEM and 250 μ M BSO for two hours. Recovery in D-Media including either 0.1 μ g/ml or 0.5 μ g/ml actinomycin D was followed by flow cytometry. ACD values are means of duplicate samples, $n > 3000$ cells, S.E.M. = 0.09 to 0.12.

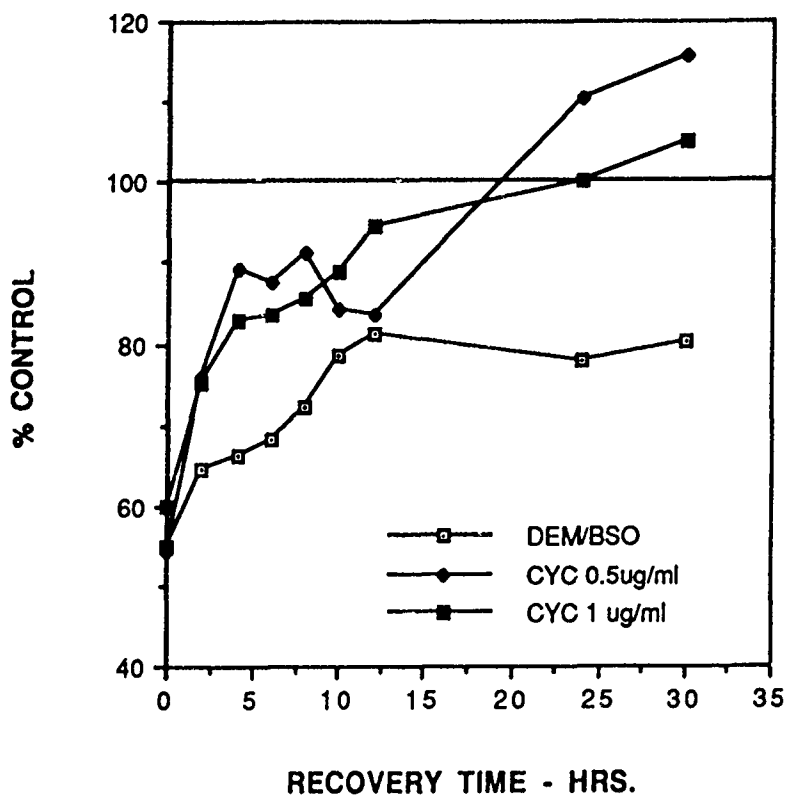


Figure 30. Cycloheximide effect on GSH recovery following BSO treatment. Cells were treated with 200 μ M DEM and 250 μ M PSO for two hours. Recovery in D-Media including either 0.5 μ g/ml or 1.0 μ g/ml cycloheximide was followed by flow cytometry. CYC values are the mean of duplicate samples drawn from parallel plates ($n > 3000$ cells each, S.E.M. = 0.001 to 0.01).

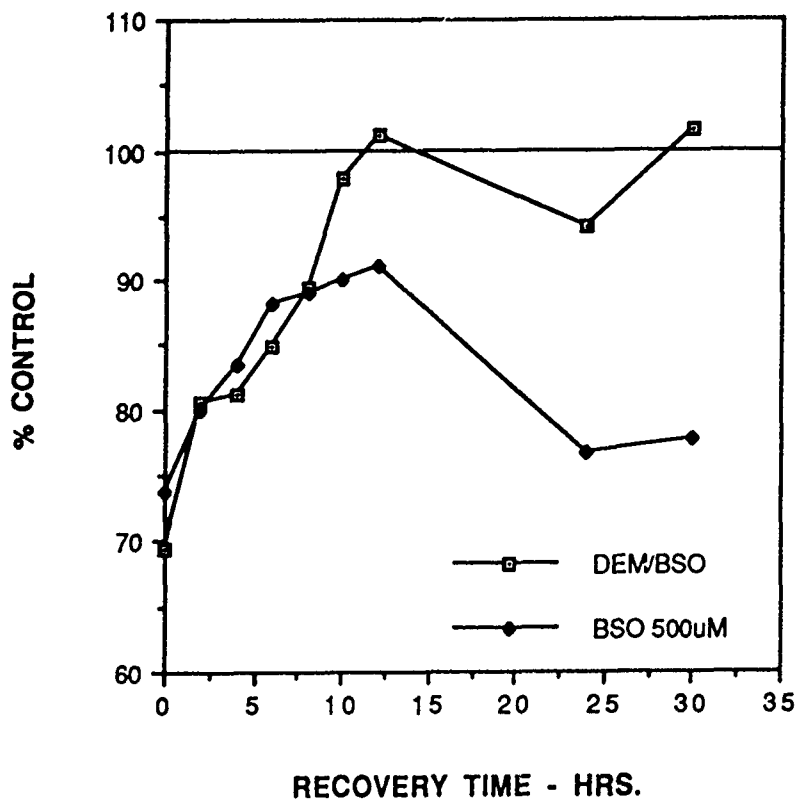


Figure 31. Effect of 500 μ M BSO on GSH recovery following BSO treatment. Cells were treated with 200 μ M DEM and 250 μ M BSO for two hours. Recovery in D-Media including 500 μ M BSO was followed by flow cytometry. Values are means of repeated samples from duplicate plates ($n > 4500$ cells each, S.E.M. = 0.001 to 0.11).

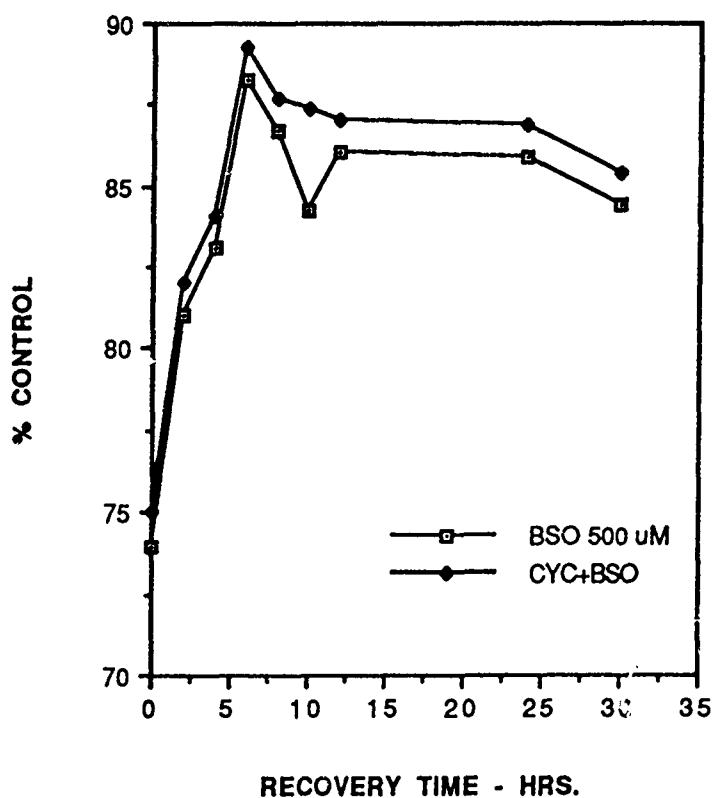


Figure 32. Cycloheximide effect on BSO inhibition. Cells were depleted with 250 μM BSO + 200 μM DEM for two hours. Replacement media contained 500 μM BSO with and without 1.0 $\mu\text{g/ml}$ CYC. Values are means of two samples from duplicate plates ($n > 2000$ cells each sample, S.E.M. = 1.10 to 0.1).

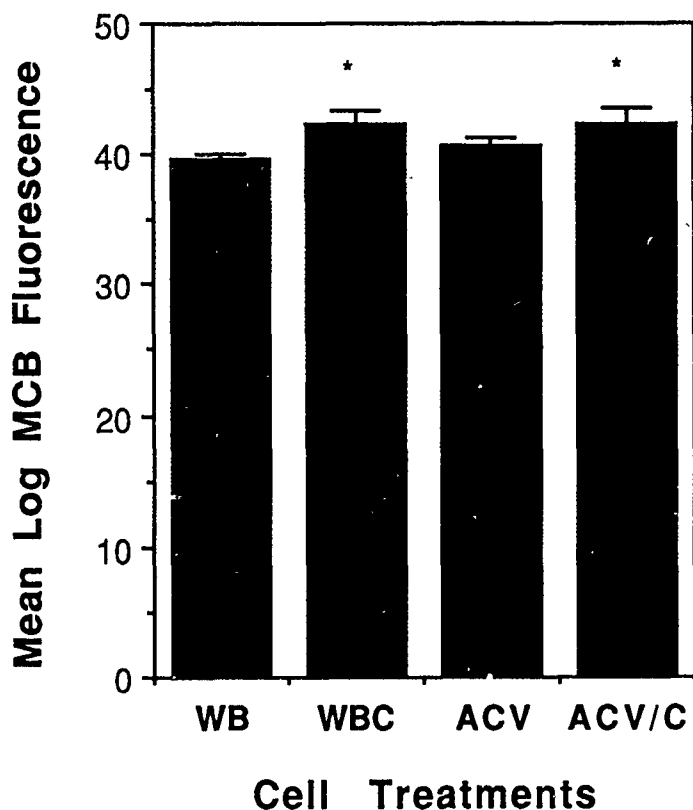


Figure 33. Acivicin effect on CYC elevation of GSH. WB = WB cells in normal media; WBC = WB in normal media containing 1 $\mu\text{g/ml}$ CYC; ACV = WB cells in media containing 50 μM acivicin; ACV/C = WB cells in media containing 50 μM acivicin + 1 $\mu\text{g/ml}$ CYC. *CYC elevated GSH levels significantly above controls ($p < 0.05$, mean of two samples, $n > 2000$ cells each, from duplicate plates). Acivicin inhibition of GGT did not modify the CYC effect.

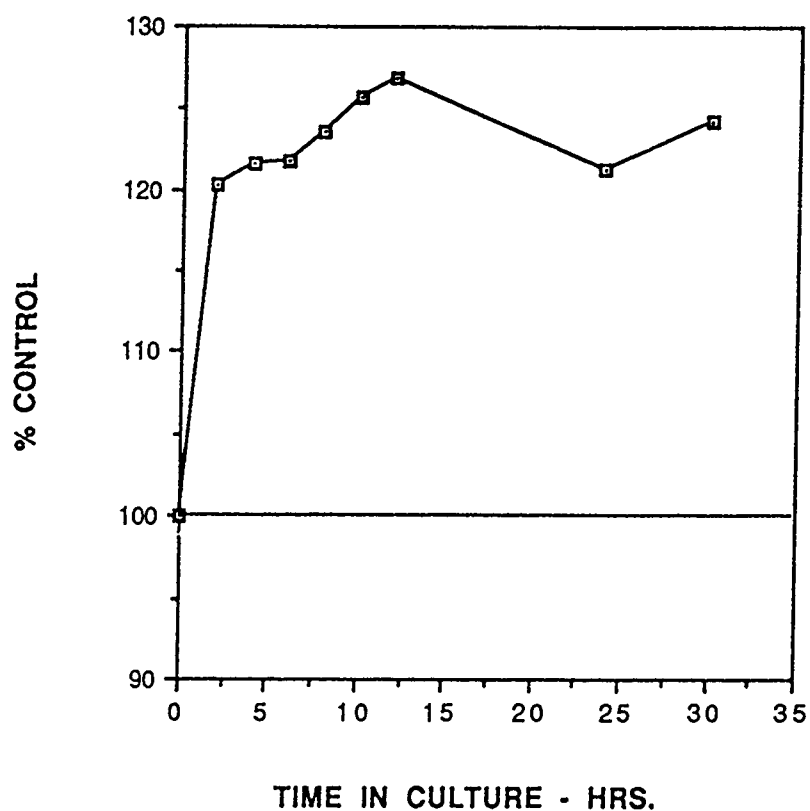


Figure 34. CYC-mediated GSH increase. Duplicate plates of WB344 cells were treated with 1.0 $\mu\text{g/ml}$ cycloheximide. GSH values were followed by flow cytometry. Each point is the mean of two samples drawn from duplicate plates ($n > 3500$ cells each sample, S.E.M. = 0.001 to 0.05).

TABLE 4 Cycloheximide effect on GSH levels in WB344 and V79 cells with normal and cystine-free (CF)[†] media.

	D-media Control	D-media + CYC	CF media	CF media + CYC
WB344	63.18±1.6	66.21±1.2** p < .005	62.14±0.4 N.S.	62.38±0.3 N.S.
V79	66.88±0.2	70.57±0.5** p < .001	71.74±0.7**	71.90±0.1 N.S. [†]

Numbers are log mean MCB fluorescence measured by flow cytometry (see methods). Each value represents the mean ± s.d. of four samples of n > 2000 cells each taken from duplicate 30 mm plates. CYC concentration = 1 µg/ml.

* CF media = D-PBS + 1 mg/ml dextrose

** significantly different from controls

† not significantly different from CF media without CYC

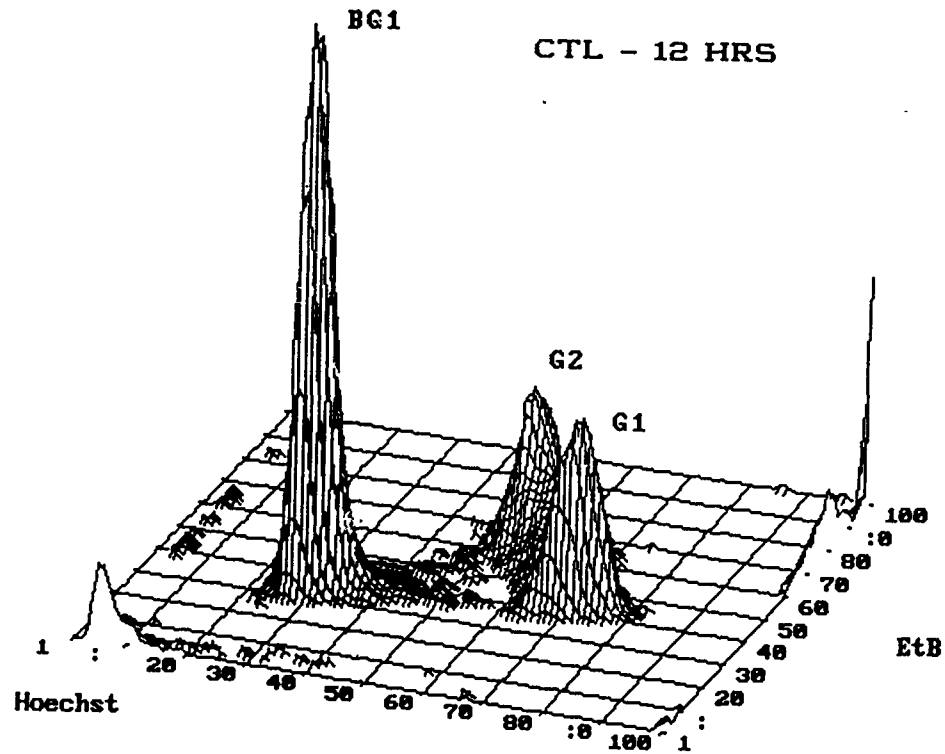


Figure 35. Control cell cycle profile - 12 hours. WB344 cells sequenced as described in methods and plated into D-media containing 100 μ M BrDU.

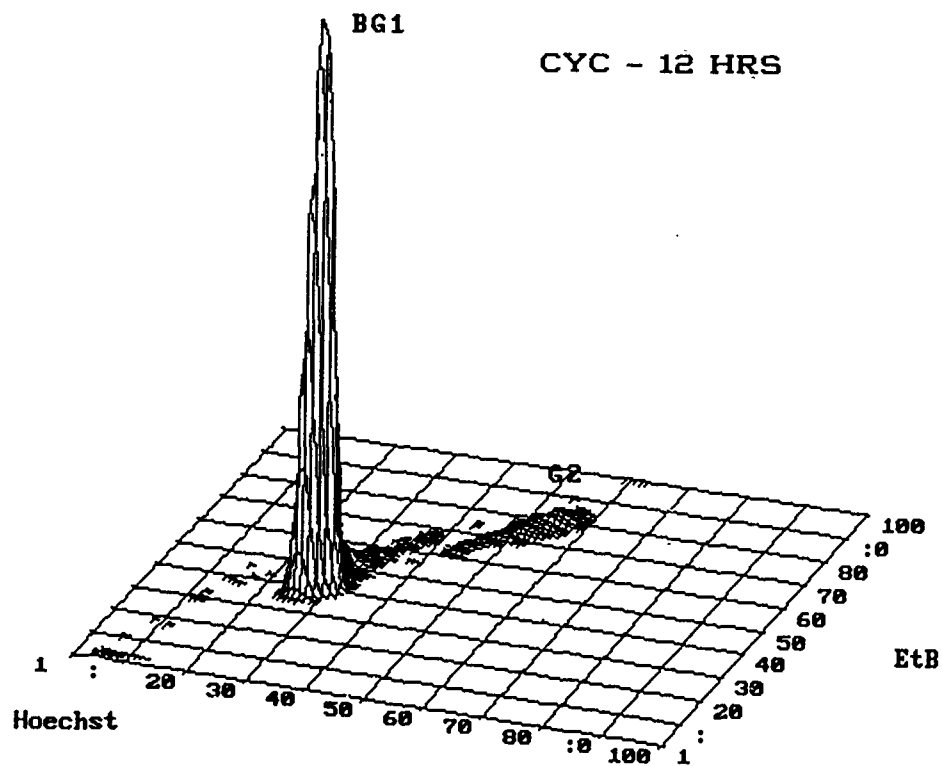


Figure 36. CYC cell cycle profile - 12 hours. WB344 cells sequenced as described in methods and plated into D-media containing 100 μ M BrDU and 1.0 μ g/ml cycloheximide.

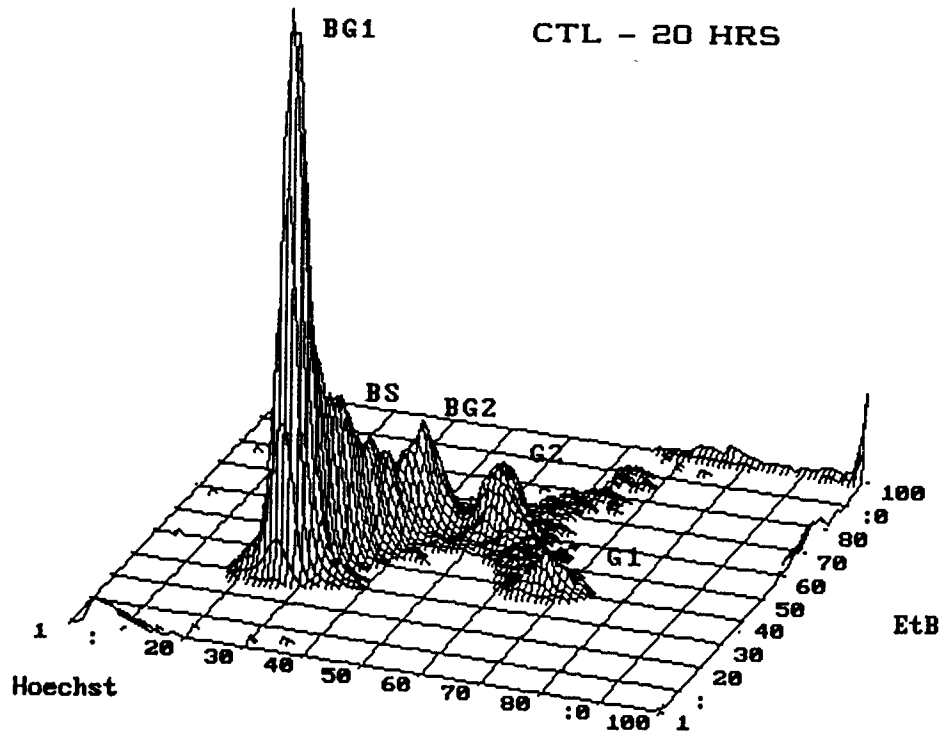


Figure 37. Control cell cycle profile - 20 hours.

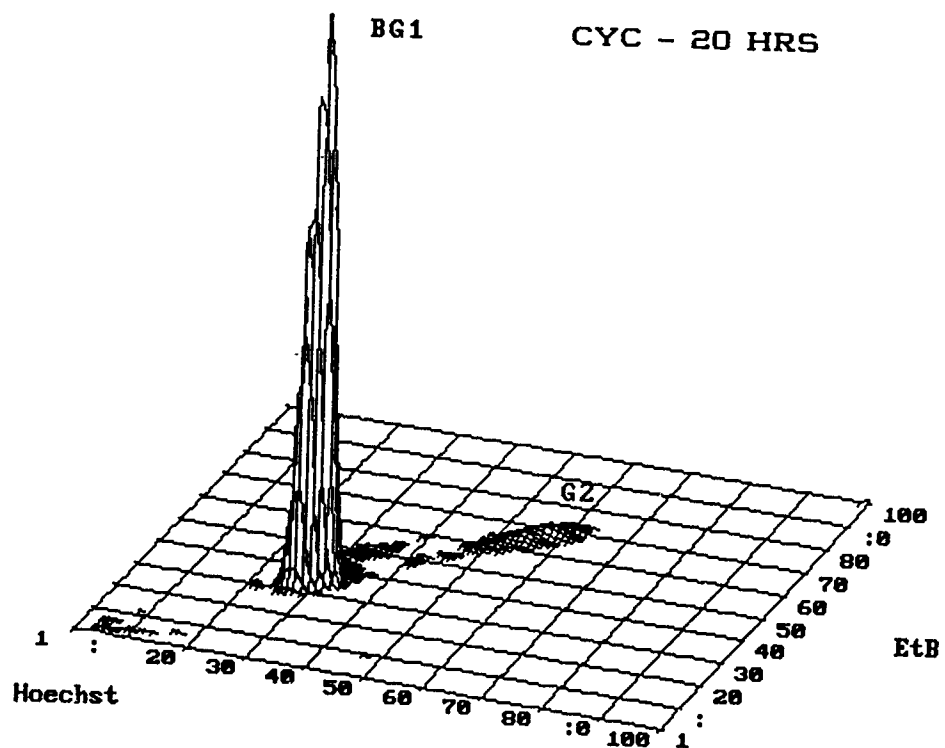


Figure 38. CYC cell cycle profile - 20 hours.

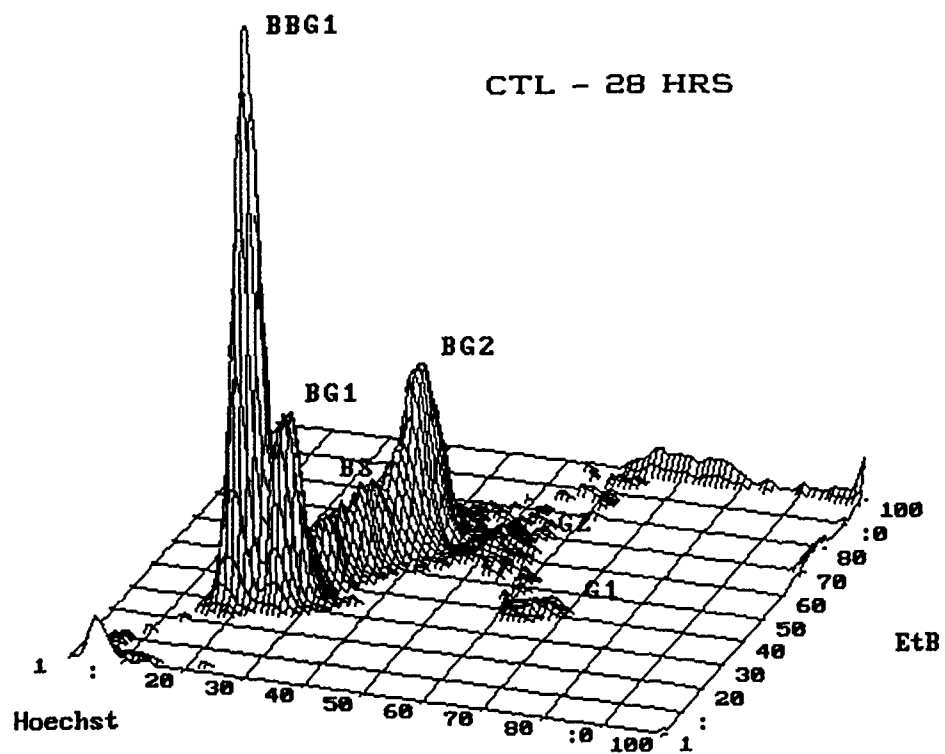


Figure 39. Control cell cycle profile - 28 hours.

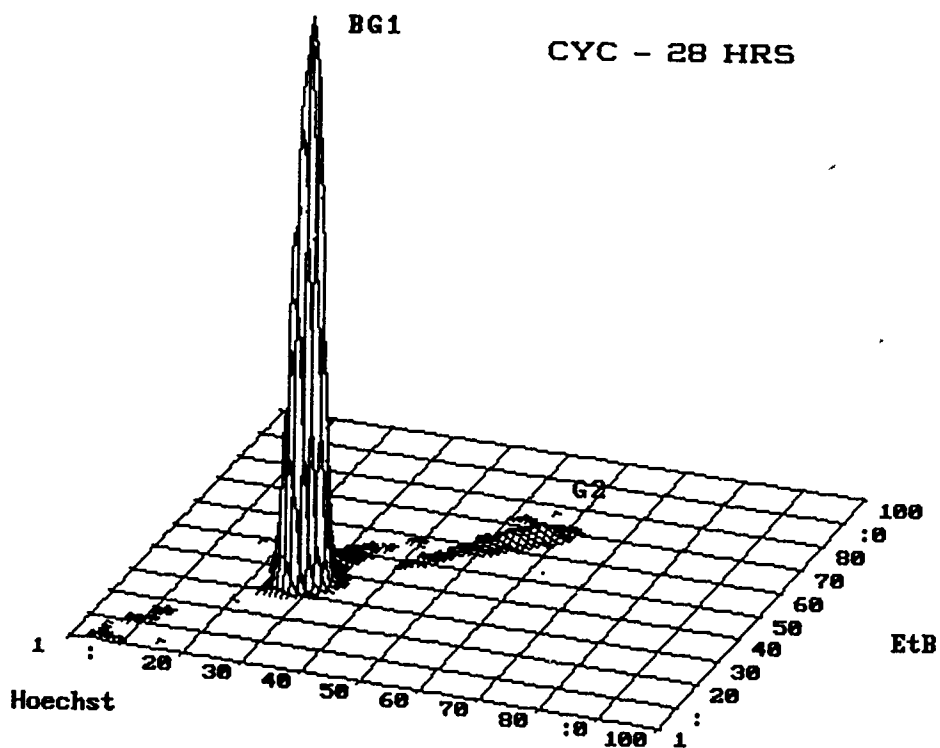


Figure 40. CYC cell cycle profile - 28 hours.

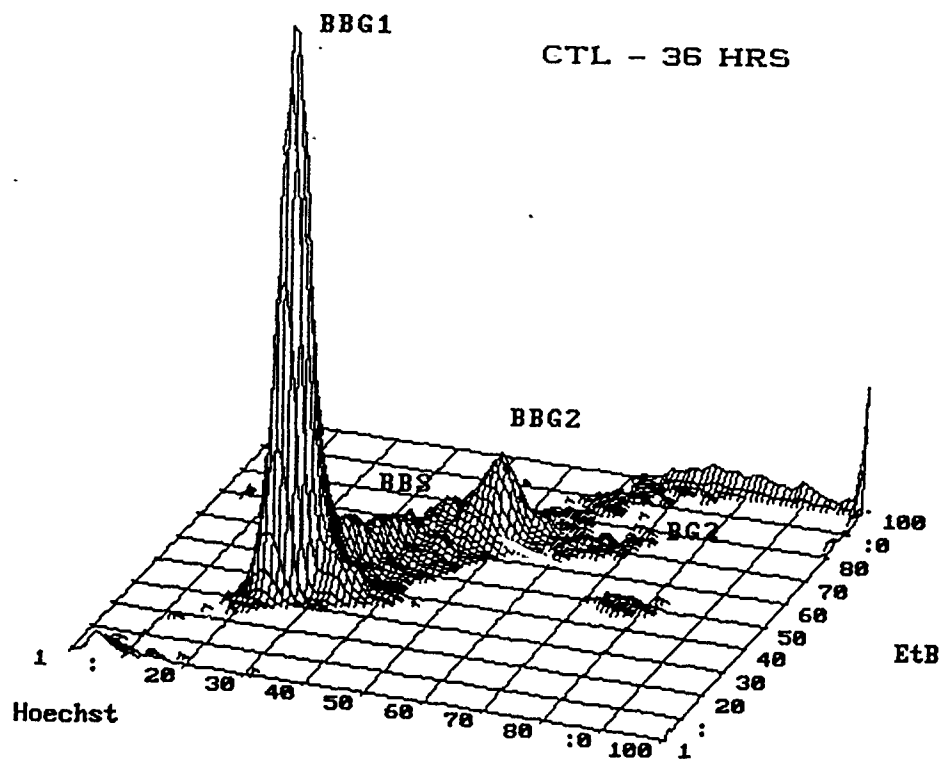


Figure 41. Control cell cycle profile - 36 hours.

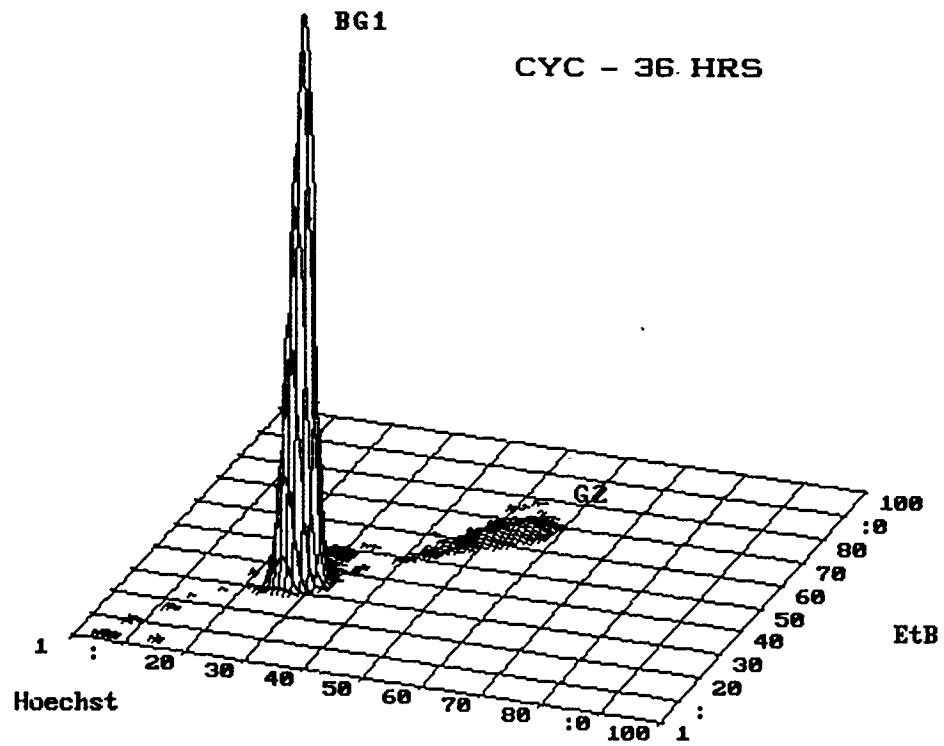


Figure 42. CYC cell cycle profile - 36 hours.

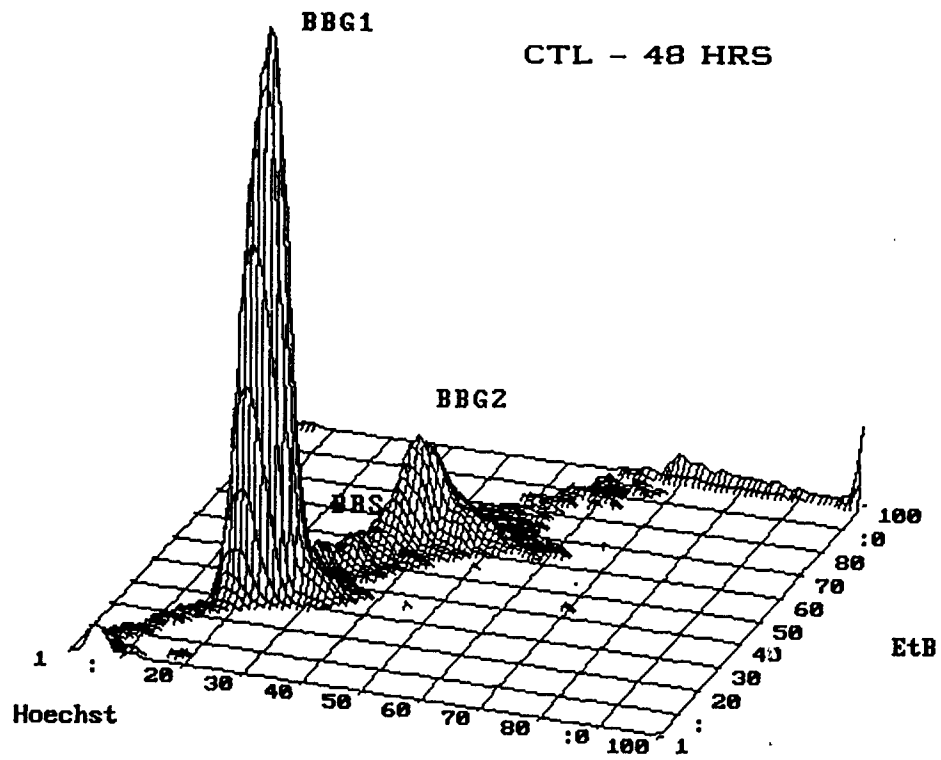


Figure 43. Control cell cycle profile - 48 hours.

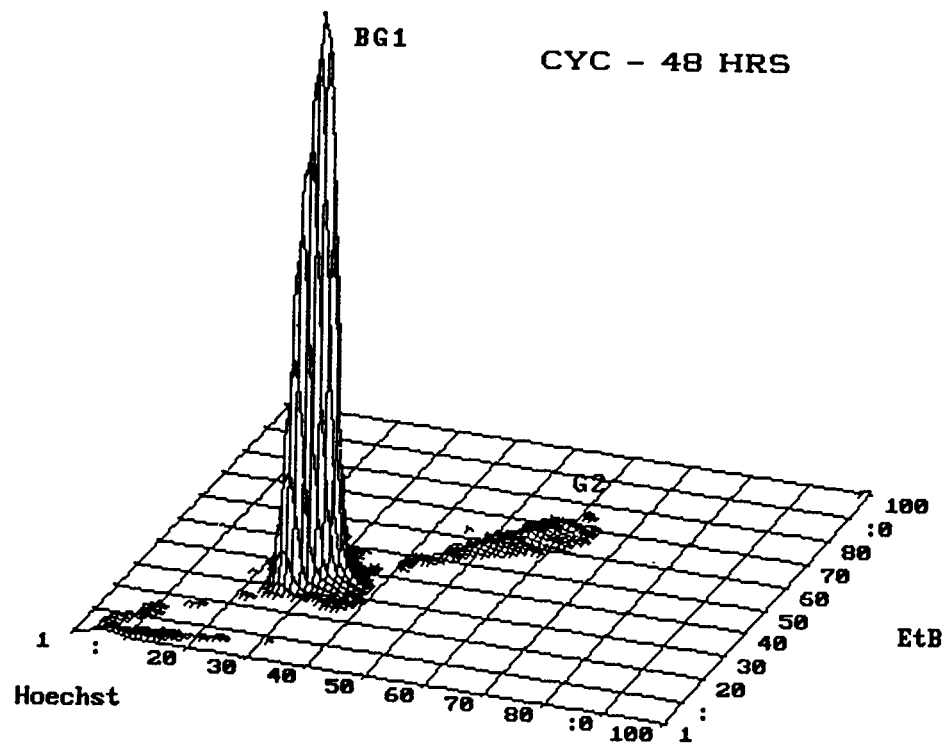


Figure 44. CYC cell cycle profile - 48 hours.

Discussion

WB344 characterization

The elusive task of definitively placing WB344 cells in the family tree of liver cells remains problematic. Results from the DES treatment study were encouraging - albumin (ALB) expression went up and AFP went down, both are phenomena expected of a "juvenile" hepatocyte growing up. During the maturation process, hepatocytes *in vivo* normally express both ALB and AFP (56); some subadult forms only express AFP (74). The DES findings support the idea that WB344(s) are either a precursor form or indeed a retrodifferentiated hepatocyte. However, since the only other parameter that we could observe as a key for maturation was morphology and since it was not the aim to settle cell origin questions, follow up on these observations was abandoned.

More to the point is that WB344(s) express all the pertinent GSH enzymes, with the possible exception of GGT which is also consistent with the phenotype of mature hepatocytes.. Moreover, they do so stably and lend themselves well to induction/inhibition studies for dissecting the biosynthesis of GSH.

Induction of γ -GCS

Many enzyme systems responsible for metabolizing xenobiotic agents respond to specific "inducers" with increased activity. Phenobarbital (PB) is classically used

as a broad spectrum inducer to elevate both the Phase I and Phase II enzyme systems. The former system is thought to be that responsible for oxidizing xenobiotics, leaving Phase II enzymes (like GST) to conjugate and detoxify the product (44). I have demonstrated that PB also increases γ -GCS activity, a finding which speculates a common regulatory element between manufacture of GSH and its utilization via GST. This is supported by the observed increase in both GST and γ -GCS by a monofunctional inducer (75) such as BHA. Just why an antioxidant such as BHA should stimulate the synthesis of an endogenous antioxidant is unclear, unless it is, in fact, a metabolite of BHA which signals for up-regulation of γ -GCS. Peroxidative activation of BHA has been demonstrated (76) and if this were the general case it becomes one more "bad actor" to be conjugated into submission - again the common signal link between GSH's birth and its use.

Selenium's effect on γ -GCS has been reported in rat liver (77) and is confirmed by my results. The method it employs to elevate that enzyme appears to be very different from PB or BHA. Selenium failed to affect GST activity in this study, a finding supported in both primary rat hepatocyte culture (42) and *in vivo* liver (78) reports. Although a necessary constituent of GSH-peroxidase (GSH-PX), selenium plays no obvious direct role in the synthesis of

GSH (15). The fact that it proved quite toxic in relatively low concentration, may indicate that disruption of cellular redox status by the obligate expenditure of two GSHs to regenerate the selenolate-enzyme is the *real* signal up-regulating γ -GCS. Since GSH levels were not elevated with selenium treatment, the scenario of an activated GSH-PX throwing itself upon some as yet unidentified peroxide substrate while gobbling up newly made GSH is plausible. That scenario could account for the seemingly paradoxical increase in γ -GCS without a corresponding elevation in GSH.

The γ -GCS expression experiments are only indirect evidence for a real elevation of that enzyme. For definitive answers, message-RNA should be measured - a prospect which, until the recent isolation of a probe against mammalian γ -GCS mRNA, would have been impossible (79).

Depletion/repletion of GSH

Transcriptional control: Why should a cell depleted of GSH rebound to levels even higher than it started with? If one assumes that *de novo* synthesis of γ -GCS may be triggered by the altered ratio between GSH and GS-protein conjugates, then the higher "overshoot" reported here is not surprising. However, the incorporation of actinomycin-D at dosages which substantially inhibit transcription of DNA, hence the manufacture of new enzyme via mRNA, fails to stop the

rebound. If the original γ -GCS is eliminated by BSO, leaving the cell no option but to make new enzyme if it wants to replenish lost GSH, ACD is still unable to prevent the gradual return to normal. Since the Theory of Spontaneous Generation fell into disfavor with Messrs. Wallace and Darwin, other possibilities must include:

BSO inhibition of γ -GCS is not irreversible: We know that, in fact, glutamate can *compete* with BSO for the active site on γ -GCS, however, once bound it appears the BSO- γ -GCS union is etched in stone (80). There is no evidence in my experiments with ACD that would support a revision of that long held view. Even if ACD were able to completely reverse BSO it still could not explain the overshoot phenomena unless one forwarded the idea that ACD also suppressed the feedback inhibition of rising GSH levels. Because of the GSH overshoot observed in my investigations and the fact that any ACD "reversal" would have been swamped by the much greater BSO concentration, I'll not speak the heresy of suggesting BSO inhibition is incompetent.

ACD dosages were insufficient to inhibit transcription: Glutathione is an ancient compound. It is one of the duties payed by pre-millennial ancestors to raise their heads out of the anaerobic ooze and into the oxygen atmosphere of a very young planet earth. Such a long established and fundamental cellular system would likely be very closely held and not subject to inhibition short of cell death. In

the repletion studies, ACD concentrations sufficient to stop transcription by over 75% were insufficient to halt production of GSH. Assuming that *de novo* γ -GCS is required to explain GSH repletion and overshoot, my results support that transcriptional regulation of the γ -GCS gene is highly conservative. It would appear to be the "Captain" of the ship, going down with his vessel only after all alternatives have failed.

De novo transcription is not required to replenish GSH: Another pathway leading to the increase in GSH would be to short circuit γ -GCS by providing its product directly to glutathione synthetase. This has been observed in tissues with high GGT levels (67,81). Most all reports discussing the WB344 cell line have indicated these cells have only low levels of GGT activity (57,59); some have used this cell line as a "negative GGT control" in expression studies (70). A report finding no GGT in fresh liver slices from Fischer 344 rats, the parental origin of WB344 cells, supports the *in vitro* findings (82). Never the less, GGT is present and some investigators have measured its activity in response to chemical challenge: Tsao *et al* (59) reported that phenobarbital treatment depressed what little GGT activity was present; another study reported that retinoic acid failed to stimulate GGT in WB344s but did elevate GGT activity in a chemically transformed cell line (60).

If GGT could be activated by some treatment, the overshoot phenomena would still lack explanation. Given the experimental procedure, the cells would have to rescue the γ -glutamyl moiety from DEM conjugation and somehow recycle it with 100% efficiency. Were that the case the return to normal GSH levels would be logical but, without some mechanism to either produce new γ -glutamyl moieties or to negate GSH inhibition of γ -GCS, overshoot GSH remain problematic.

Translational control: The converse of the preceding argument, this concept is not without example. Tubulin, the cytoplasmic constituent responsible for the microtubules of cell division, is regulated at the translational level (79,81). This is not the norm; most enzymes are regulated by modifying gene transcription (15).

Far and away the biggest surprise of these experiments was the effect that cycloheximide had on GSH levels. Classically used as an inhibitor of protein synthesis, cycloheximide acts to stop nascent protein chain elongation and to prohibit chain initiation by halting polysome reaggregation (83). At the levels used in my studies, CYC inhibited protein synthesis by greater than 90%, and yet it failed to stop GSH overshoot or repletion. In fact, CYC itself increased GSH levels far above controls. In the BSO treatment repletion studies, CYC accelerated the recovery of

GSH and even surpassed control values within 30 hours. Clearly this result argues against the necessity of new protein synthesis for GSH recovery.

A report by Tateishi *et al* (84) supports the conclusion that *de novo* synthesis of γ -GCS is not required for GSH recovery from depleted levels. In their *in vivo* feeding studies both ACD and CYC failed to inhibit recovery of GSH to normal upon feeding of starved rats. The authors report that CYC actually increased hepatic GSH in both starved and fed rats.

Cycloheximide

The observation that CYC could elevate GSH has been reported; Freedman *et al* (17) observed the effect in a rat hepatoma cell line, Deneke *et al* (4) described it in endothelial cells and, as described above, Tateishi (84) confirmed a GSH elevation by CYC independent of feeding status in rats.

Cycloheximide has some interesting effects on cellular transport systems as well. Radiolabeled GSH experiments indicate that CYC enhances intestinal absorption of GSH and its transport to plasma (35). Cycloheximide inhibits protein secretion by isolated hepatocytes but did not attack components of the secretory mechanism itself apart from depressing *de novo* protein synthesis (85), suggesting that CYC may reduce the level of certain regulatory proteins.

Deneke speculated this "protein signaling" might explain GSH elevations; cell transport systems for precursor amino acids may be repressed by some as yet unidentified protein which is effectively removed by CYC (1). The data from the normal vs. "cystine free" media experiment indicate that transport of *some* extracellular component is linked to cycloheximide's effect. Aside from inorganic salts present at physiological levels and dextrose, D-PBS media contained no amino acids which could be incorporated into new intracellular GSH. Normal media, with its full complement of amino acids allowed the CYC-mediated GSH increase. Cysteine (via cystine) is most likely the constituent responsible as it is the substrate in lowest supply in serum (1,2). Activation of the cystine-specific transporter (X_c^-) by low concentrations of DEM can elevate cellular GSH in several cell types (86). Other electrophilic agents such as sulfobromophthalein strongly induce the X_c^- transporter in hepatocytes (5). If CYC activates this transporter directly or through reduction of a repressor protein, cellular GSH could be expected to rise. Finally, the acivicin experiment data fairly rule out a cycloheximide-stimulated GGT-mediated import of γ -glutamyl cysteine moieties which could bypass γ GCS; CYC elevated GSH in the face of specific GGT inhibition.

Still, CYC-stimulated cystine transport may only partially explain elevated GSH; some mechanism must

eliminate the feedback inhibition those increasing GSH levels would have on γ -GCS to allow the higher than normal values we have seen. There is nothing in CYC's structure (figure 45) to support its direct intervention in the affairs of BSO inhibition. It lacks both the thiol and the glutamate analogue required to bind at the active site of γ -GCS (13).

Cycloheximide's effect on cell cycling is even more interesting. The entire population of synchronized cells is rushed through one mitosis and stalls in BG1, the presynthetic phase of the second cell cycle. This would appear to be a mechanistic alteration which is not particularly toxic to the cell; cell death is not significantly different from control cells. One possible explanation is that protein constituents necessary for synthesis are "used up" and not resynthesized under CYC influence. The elevated GSH levels accelerate the completion of first cell division by pushing nucleotide and polymerase action, possibly through the swift elimination of oxidized byproducts which under normal circumstances would moderate the speed of division. Energy in the form of ATP would be sufficient to sustain this scenario as CYC had been demonstrated not to significantly interfere with mitochondrial protein synthesis (87) or energy metabolism, even at high concentrations (88).

Figure 45 summarizes the possible routes through which cycloheximide may act to produce elevated intracellular GSH and accelerated cell cycling. Central to the scheme is CYC's modification of cellular redox status. CYC, a β hydroxyketone, readily loses H_2O to become an α, β unsaturated ketone with an exocyclic double bond (89). This form is very reactive with thiols and may account for its inhibition of protein synthesis by adducting with initiation/elongation factors. It is no long stretch of logic to presume its reactivity with the most prevalent cellular thiol, glutathione. It at first blush seems paradoxical that CYC may initially deplete GSH but, in so doing the GSH/GSSG ratio is altered, a situation which has been linked to control of protein synthesis in its own right (89,90). The initial depletion could then be reversed in a redox regulated synthesis phase analogous to "supply side" economics.

If cyc indeed alters the redox status several consequences follow. Several "stress proteins" are expressed *de novo* under oxidative challenge some of which are protective (34). GSH, GS-protein conjugates and GSSG have been shown to participate directly in the induction of stress proteins (30,31,33). These reports are consistent with the conclusion that the GSH/GSSG ratio is a regulatory mechanism which stimulates protective strategies and

inhibits "nonessential" synthesis. It represents a "circle the wagons" approach in cellular defense strategy.

As previously mentioned, transport systems responsible for accumulating GSH precursors are also stimulated by some oxidants (1). GSH/GSSG ratio changes are linked to increased transport activity (80). Cycloheximide conceivably uses modification of that ratio to induce or suppress regulatory proteins which: a) enhance substrate transport of GSH precursors and, b) modify GSH feedback inhibition of γ -GCS. Upon reflection, the GSH/GSSG ratio is by analogy the cell's military force -- in time of peace not much thought of, but once under attack it becomes vital.

Conclusions

This project has demonstrated that the WB344 cell line is a stable test bed for study of some aspects of cellular redox events. Its phenotype and reaction to various test agents validate it as a suitable *in vitro* model of untransformed hepatocytes.

I have demonstrated that γ -GCS may be induced by several chemical treatments representing gene regulatory sites which are possibly shared with both phase I and phase II xenobiotic metabolizing systems. Further, if γ -GCS gene expression is induced by specific cis or trans-acting elements, it is highly conserved and only stops with cell

death. A time course experiment with CYC measuring GSH and γ GCS-mRMA would definitively answer this speculation.

Finally, cycloheximide studies indicate that cellular redox, probably acting through GSH/GSSG ratios triggers protective mechanisms which act in concert to re-establish physiologic homeostasis. One such mechanism appears to be a strong stimulation of cellular transport systems which are responsible for acquiring GSH precursor amino acids.

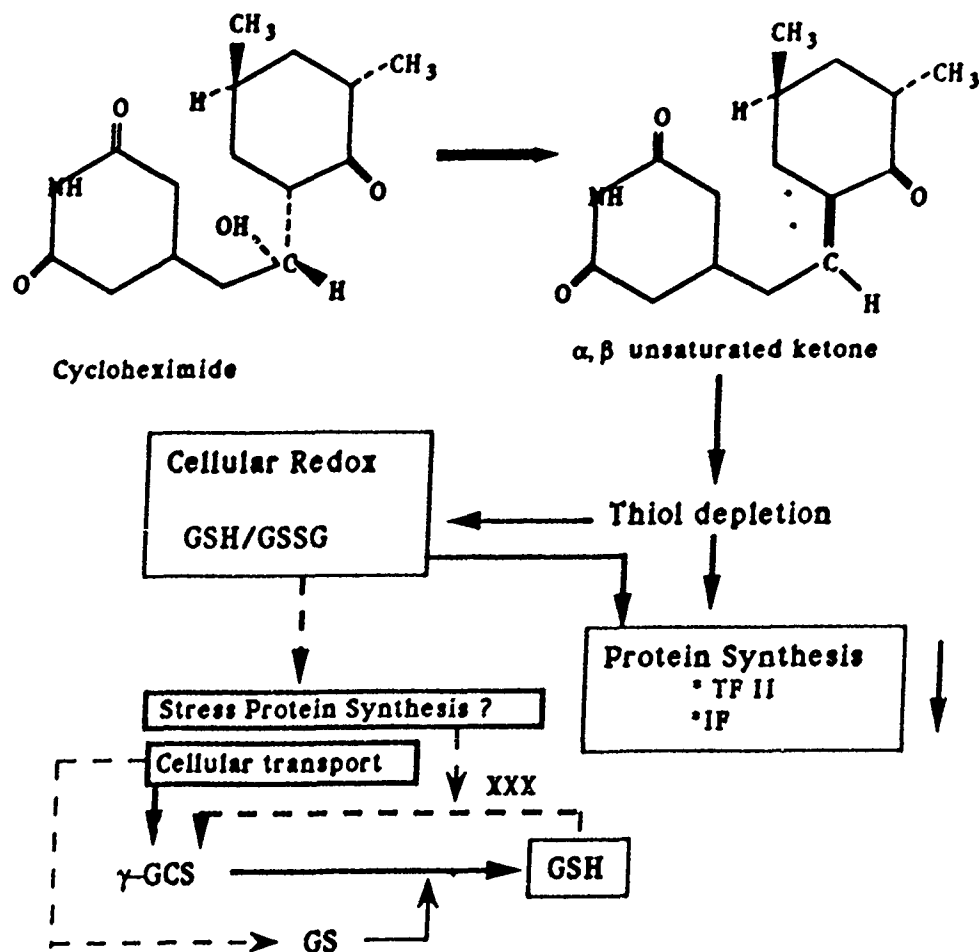


Figure 45. Cycloheximide structure activity and possible mechanisms. CYC readily loses H_2O to form a thiol-reactive unsaturated ketone. Through direct interaction on protein synthesis initiation factors (IF) or aminoacyl transferase II (TF II), general protein synthesis is inhibited. Modification of cellular redox may initiate a poorly characterized group of "stress proteins" which may serve to upregulate cell defense systems. The stress proteins could conceivably exist in "apoprotein" form and are cleaved to activity by altered GSH/GSSG or GS-protein conjugate action.

REFERENCES

1. Deneke, S.M. and Fanburg, B.L., Regulation of Cellular Glutathione. *Amer. J. Physio.* 257(4P+1): L 163-173, (1989).
2. Bannai, S. and Tateishi, N., Role of Membrane Transport in Metabolism and Function of Glutathione in Mammals. *J. Membrane Biol.* 89 1-8, (1986).
3. Bannai, S., Induction of Cystine and Glutamate Transport Activity in Human Fibroblasts by Diethyl Maleate and Other Electrophilic Agents. *Journal of Biological Chemistry* 259: 2435-2440, (1984).
4. Deneke, S.M., Baxter, D.F., Phelps, D.T., and Fanburg, B.L., Increase in Endothelial Cell Glutathione and Precursor Amino Acid Uptake by Diethyl Maleate and Hyperoxia. *The American Physiological Society* 1040-0605: L265-271, (1989).
5. Bannai, S., Takada, A., Kasuga, H., and Tateishi, N., Induction of Cystine Transport Activity in Isolated Rat Hepatocytes by Sulfobromophthalein and Other Electrophilic Agents. *Hepatology* 6 1361-1368, (1986).
6. Watanabe, H. and Bannai, S., Induction of Cystine Transport Activity in Mouse Peritoneal Macrophages. *J. Exp. Med.* 165: 628-640, (1987).
7. Meister, A., New Aspects of Glutathione Biochemistry and Transport: Selective Alteration of Glutathione Metabolism. *Federation Proceedings* 43: 3031-3042, (1984).
8. Reed, D.J. and Beatty, P.W., Biosynthesis and Regulation of Glutathione: Toxicological Implications. *Reviews in Biochemical Toxicology* 2: 213-240. (1979).
9. Kosower, N. and Kosower, E., Glutathione Status of Cells. *International Review of Cytology* 54: 109-160. (1978).
10. Stenius, U. and Högberg, J., GGT Resistance. *Carcinogenesis* 9: 1223-1227, (1988).
11. Sell, S. and Leffert, H.L., An Evaluation of Cellular Lineages in the Pathogenesis of Experimental Hepatocellular Carcinoma. *Hepatology* 2: 77-86, (1982).

12. Richman, P.G. and Meister, A., Regulation of γ -Glutamyl-Cysteine Synthetase by Nonallosteric Feedback Inhibition by Glutathione. *The Journal of Biological Chemistry* 250: 1422-1426, (1975).
13. Huang, C-S, Moore, W.R., and Meister, A., On the active site thiol of γ -glutamylcysteine synthetase: Relationships to catalysis, inhibition, and regulation. *Proc. Natl. Acad. Sci. USA* 85: 2464-2468, (1988).
14. Drew, R. and Miners, J., The Effects of Buthionine Sulphoximine (BSO) on Glutathione Depletion and Xenobiotic Biotransformation. *Biochemical Pharmacology* 33: 2989-2994, (1984).
15. Stryer, L. Biochemistry. 3 ed. W.H. Freeman and Co., NY. pp. 592-593. (1988).
16. Taylor, Y.C. and Brown, J.M., Elevation of Intracellular Glutathione Levels Following Depletion and Its Relationship to Protection Against Radiation and Alkylating Agents. *Pharmac. Ther.* 39: 293-299, (1988).
17. Freedman, J.H., Ciriolo, M.R., and Peisach, J., The Role of Glutathione in Copper Metabolism and Toxicity. *The Journal of Biological Chemistry* 264: 5598-5605, (1989).
18. Rotstein, J.B. and Slaga, T.J., Effect of Exogenous Glutathione on Tumor Progression in the Murine Skin Multistage Carcinogenesis Model. *Carcinogenesis* 9: 1547-1551, (1988).
19. Boyer, T.D., The Glutathione S-Transferase: An Update. *Hepatology* 9: 486-496, (1989).
20. Pearson, W.R., Reinhart, J., Sisk, S.C., and Anderson, K.S., Tissue-specific Induction of Murine Glutathione Transferase. *Journal of Biological Chemistry* 263: 13324-13332, (1988).
21. Kalinyak, J.E., and Taylor, J.M., Rat Glutathione S-Transferase. *Journal of Biological Chemistry* 257: 523-530, (1982).
22. Morrow, C.S., Cowan, K.H., and Goldsmith, M.E., Structure of the human genomic GST. *Gene* 75: 3-11, (1989).

23. Moscow, J.A., Townsend, A.J., Goldsmith, M.E., Whang-Peng, J., Vickers, P.J., Poisson, R., Legault-Poisson, S., Myers, C.E. and Cowan, K.H., Isolation of the human anionic GST DNA. *Proc. Natl. Acad. Sci. USA* 85: 6518-6522, (1988).
24. Abramovitz, M. and Listowsky, I., Development regulation of glutathione S-transferases. *Xenobiotica* 18: 1249-1254, (1988).
25. Bauman, P.F., Smith, T.K. and Bray, T.M., Effect of Dietary Protein Deficiency and L-2-oxothiazolidine-4-carboxylate on the diurnal rhythm of hepatic glutathione in the rat. *J. Nutr.* 118:1048-1054, (1988).
26. Sakai, M., Okuda, A., and Muramatsu, M., Multiple regulatory elements-GST. *Proc. Natl. Acad. Sci. USA* 85: 9456-9460, (1988).
27. Lewis, A.D., Hickson, I.D., Hobson, C.N., Harris, A. L., Hayes, J.D., Griffiths, S.A., Manson, M.M., Hall, A.E, Moss, J.E., and Wolf, C.R., Amplification and increased expression of GST genes. *Proc. Natl. Acad. Sci. USA* 85: 8511-8515, (1988).
28. Aniya, Y. and Anders, M.W., Activation of Rat Liver Microsomal GST. *Journal of Biological Chemistry* 264: 1998-2002, (1989).
29. Aniya, Y. and Anders, M.W., Regulation of Rat Liver Microsomal GST Activity. *Archives of Biochemistry and Biophysics* 270: 330-334, (1989).
30. Bellomo, G., Mirabelli, F., DiMonte, D., Richelmi, P., Thor, H., Orrenius, C., and Orenius, S., Formation and Reduction of Glutathione-Protein Mixed Disulfides During Oxidative Stress. *Biochemical Pharmacology* 36: 1313-1320, (1987).
31. Freeman, M. and Meredith, M., Glutathione Conjugation and Induction of a 32,000 Dalton Stress Protein. *Biochemical Pharmacology* 38: 299-304, (1989).
32. Keyse, S.M. and Tyrrell R.M., Both Near Ultraviolet Radiation and the Oxidizing Agent Hydrogen Peroxide Induce a Stress Protein. *Journal of Biological Chemistry* 262: 14821-14825, (1987).

33. Shelton, K., Egle, P., and Todd, J., Evidence that Glutathione Participates in the Induction of a Stress Protein. *Biochemical and Biophysical Research Communication* 134: 492-498, (1986).
34. Christman, M.F., Morgan, R.W., Jacobson, F.S., and Ames, B.N. *Cell* 41: 753-762, (1985).
35. Yassuhiko, K. Absorption of ^{35}S -GSH and its incorporation into protein in rats. *Kurume Med. J.* 15:113-125, (1968).
36. Grisham, J.W., Use of Hepatic Cell Cultures to Detect and Evaluate the Mechanisms of Action of Toxic Chemicals. *International Review of Experimental Pathology* 20: 123-210, (1979).
37. Bissell, D.M., Study of Hepatocyte Function in Cell Culture. Progress in Liver Disease Vol V. Chp. 5, Grune & Stratton, NY. pp.69-82. (1976).
38. Kera, Y., Penttilä, K. and Lindros, K., Glutathione replenishment capacity is lower in isolated perivenous than in periportal hepatocyte. *Biochem. J.* 254: 411-417, (1988).
39. Fahl, W.E., Michalopoulos, G., Sattler, G., Jefcoate, C., and Pitot, H., Characteristics of Microsomal Enzyme Controls in Primary Cultures of Rat Hepatocyte. *Archives of Biochemistry and Biophysics* 192: 61-72, (1979).
40. Burt, R., Garfield, S., Johnson, K. and Thorgeirsson, S., Transformation of rat liver epithelial cells. *Carcinogenesis* 9: 2329-2332, (1988).
41. Meyer, D.J., and Ketterer, B., Glutathione transferase isoenzymes in cultured rat hepatocytes. *Biochemical Pharmacology* 37: 2482-2485, (1988).
42. Vandenberghe, Y., Ratanasavanh, D., Glaise, D., and Guillouzo, A., Influence of medium composition and culture conditions. *In Vitro Cellular & Developmental Biology* 24: 281-288, (1988).
43. Abramovitz, M., Ishigaki, S., and Listowsky, I., Differential Regulation of GST in Cultured Hepatocytes. *Hepatology* 9: 235-239, (1989).

44. Croci, T. and Williams, G.M., Activities of Several Phase I and Phase II Xenobiotic Biotransformation enzymes in Cultured Hepatocytes from Male and Female Rats. *Biochemical Pharmacology* 34: 3029-3035, (1985).
45. Rogiers, V., Vandenberghe, Y., Callaerts, A., Sonck, W., Maes, V., and Vercruyssen, A., The inducing and inhibiting effects of sodium valproate. *Xenobiotica* 18: 665-673, (1988).
46. Guzelian, P.S., Bissell, M., and Meyer, U.A., Drug Metabolism in Adult Rat Hepatocytes. *Journal of American Gastroenterological Association* 72: 1232-1239, (1977).
47. Armato, U., Andreis, P.G. and Romano, F., Exogenous Cu, Zn-superoxide Dismutase Suppresses the Stimulation of Neonatal Rat Hepatocytes' Growth by Tumor Promoters. *Carcinogenesis* 5: 1547-1555, (1984).
48. Miyazaki, M., Utsumi, K., and Sato, J., Mechanisms Responsible for Long-Term Survival of Adult Rat Hepatocytes in the Presence of Phenobarbital in Primary Culture. *Experimental Cell Research* 182: 415-424, (1989).
49. Inoue, C., Yamamoto, H., Nakamura, T., Ichihara, A., and Okamoto, H., Nicotinamide prolongs survival of primary cultured hepatocyte without involving loss of hepatocyte-specific functions. *Journal of Biological Chemistry* 264: 4747-4750, (1989).
50. Isom, H.C., Secott, T., Georgoff, I., Woodworth, C., and Mummaw, J., Maintenance of differentiated rat hepatocytes in primary culture. *Proc. Natl. Acad. Sci. USA* 82: 3252-3256, (1985).
51. Lee, G-H., Sawada, N., Mochizuki, Y., Nomura, K., and Kitagawa, T., Immortal Epithelial Cells of Normal C3H Mouse Liver in Culture: Possible Precursor Populations for Spontaneous Hepatocellular Carcinoma. *Cancer Research* 49: 403-409, (1989).
52. Germain, L., Blouin, M-J., and Marceau, N., Biliary Epithelial and Hepatocytic Cell Lineage Relationships in Embryonic Rat Liver as Determined by the Differential Expression of Cytokeratins, α -Fetoprotein, Albumin, and Cell Surface-exposed Components. *Cancer Research* 48: 4909-4918, (1988).

53. Mayer, D. and Schäfer, B., Biochemical and Morphological Characterization of Glycogen-Storing Epithelial Liver Cell Lines. *Experimental Cell Research* 138: 1-14, (1982).
54. Idoine, J.B., Elliott, J.M., Wilson, M.J., and Weisburger, E. K., Rat Liver Cells in Culture: Effect of Storage, Long-term Culture, and Transformation on some Enzyme Levels. *In Vitro* 12: 541-553, (1976).
55. Williams, G.M., Weisburger, E. K. and Weisburger, J. H., Isolation and Long-Term Cell Culture of Epithelial-Like Cells from Rat Liver. *Experimental Cell Research* 69: 106-112, (1971).
56. Sell, S., Hunt, J.M., Knoll, B.J., and Dunsford, H. A., Cellular Events During Hepatocarcinogenesis in Rats and the Question of Premalignancy. *Advances in Cancer Research* 48: 37-111, (1987).
57. Tsao, M-S., Smith, J.D., Nelson, K.G., and Grisham, J. W., A Diploid Epithelial Cell Line from Normal Adult Rat Liver with Phenotypic Properties of 'Oval' Cells. *Experimental Cell Research* 154: 38-52, (1984).
58. Tsao, M-S. and Liu, C., Inhibition of Growth of Early Passage Normal Rat Liver Epithelial Cell Lines by Epidermal Growth Factor. *Laboratory Investigation* 58: 636-642, (1988).
59. Tsao, M-S., Nelson, K. G., and Grisham, J. W., Biochemical Effects of 12-O-Tetradecanoylphorbol-13-Acetate, Retinoic Acid, Phenobarbital, and 5-Azacytidine on a Normal Rat Liver Epithelial Cell Line. *Journal of Cellular Physiology* 121: 1-6, (1984).
60. Tsao, M-S. and Batist, G., Induction of Gamma-Glutamyl Transpeptidase Activity by All-Trans Retinoic Acid in Cultured Rat Liver Epithelial Cells. *Biochemical and Biophysical Research Communications* 157: 1039-1045, (1988).
61. Evans, M., El-Fouly, M., Trosko, J., and Sleight, S., Anchored Cell Analysis/Sorting Coupled with the Scrape-Loading/Dye-Transfer Technique to Quantify Inhibition of Gap-Junctional Intercellular Communication in WB-F344 Cells by 2,2', 4,4' , 5,5' -Hexabromobiphenyl. *Journal of Toxicology and Environmental Health* 24: 261-271, (1988).

62. Kavanagh, T.J., Rubinstein, C., Liu, P.L., Chang, C.-C., Trosko, J.E., and Sleight, S.D., Failure to Induce Mutations in Chinese Hamster V79 Cells and WB Rat Liver Cells. *Toxicology and Applied Pharmacology* 79: 91-98, (1985).
63. Shapiro, H.M. Practical Flow Cytometry. 2 ed. Alan R. Liss, Inc., NY. p. 136. (1988).
64. Luna, L.G., ed. Manual of Histologic Staining Methods of the Armed Forces Inst. of Pathology. 3 ed. pp.36-39. McGraw-Hill, NY. (1968).
65. Monroe, D. and Eaton, D., Effects of Modulation of Hepatic Glutathione on Biotransformation and Covalent Binding of Aflatoxin B₁ to DNA in the Mouse. *Toxicology and Applied Pharmacology* 94: 118-127, (1988).
66. Hamel, D.M., White, C. and Eaton, D.L. Determination of γ -glutamylcystein synthetase and glutathione synthetase activity by HPLC. (submitted) May, (1990).
67. Grossmann, A., Maher, V.M. and McCormick, J.J. The frequency of mutants in human fibroblasts UV-irradiated at various times during S-phase suggest that genes for thioguanine and diphtheria toxin-resistance are replicated early. *Mutat. Res.* 152:67-76. Oct (1985).
68. Rabinovitch, P., Kubbies, M., Chen., Y., Schindler, D., and Hoehn, H., BrdU-Hoechst Flow Cytometry: A Unique Tool for Quantitative Cell Cycle Analysis. *Experimental Cell Research* 174: 309-318, (1988).
69. Rabinovitch, P., Regulation of Human Fibroblast Growth Rate by Both Noncycling Cell Fraction and Transition Probability is Shown by Growth in 5-Bromodeoxyuridine Followed by Hoechst 33258 Flow Cytometry. *Proc. Natl. Acad. Sci. USA* 80: 2951-2955, (1983).
70. Tsao, M-S, Duong, M., and Batist, G., Glutathione and Glutathione S-Transferases in Clones of Cultured Rat Liver Epithelial Cells that Express Varying Activity of γ -Glutamyl Transpeptidase. *Molecular Carcinogenesis* 2: 144-149, (1989).
71. Jones, S., Idle, J. and Hirom, P., Differential expression of glutathione transferase by native and cultured human lymphocytes. *Biochemical Pharmacology* 37: 4586-4590, (1988).

72. Vandenberghe, Y., Morel, F., Foriers, A., Ketterer, B., Vercruysse, A., Guillouzo, A., and Rogiers, V., Effect of Phenobarbital on the Expression of Glutathione S-transferase Isoenzymes in Cultured Rat Hepatocytes. *FEBS Letters* 251: 59-64, (1989).
73. Pickett, C.B., and Lu, A.Y.H., Glutathione S-Transferases: Gene Structure, Regulation, and Biological Function. *Annu. Rev. Biochem.* 58: 743-764, (1989).
74. Weber, A., Le Provost, E., Boissard-Rissel, M., Berges, J., Schapira, F. and Guillouzo, A., Localization of Fetal Aldolases During Early Stages of Azo-Dye Hepatocarcinogenesis in Rat. *Biochemical and Biophysical Research Communications* 92: 591-597, (1980).
75. Talalay, P., DeLong, M.J., and Prochaska, H.J., Identification of a Common Chemical Signal Regulating the Induction of Enzymes that Protect Against Chemical Carcinogenesis. *Pro. Natl. Acad. Sci., USA* 85: 8261-8265, (1988).
76. Thompson, D.C., Chao, Y-N, and Trush, M.A., The Peroxidase-dependent Activation of Butylated Hydroxyanisole and Butylated Hydroxytoluene (BHT) to Reactive Intermediates. *The Journal of Biological Chemistry* 264: 3957-3965, (1989).
77. Chung, A-S and Maines, M.D., Effect on Selenium on Glutathione Metabolism: Induction of γ -Glutamylcysteine Synthetase and Glutathione Reductase in the Rat Liver. *Biochemical Pharmacology* 30: 3217-3223, (1981).
78. Simplicio, P. and Leonzio, C., Effects of Selenium and Mercury on Glutathione and Glutathione-Dependent Enzymes in Experimental Quail. *Bull. Environ. Contam. Toxicol.* 42: 15-21, (1989).
79. Meister, A. Amino acid sequence of rat kidney γ -Glutamylcysteine Synthetase. *J. Biol. Chem.* 265:1588, (1990).
80. Issels, R.D., Nagele, A., Eckert, K., Wilmanns, W., Promotion of cystine uptake and its utilization for glutathione biosynthesis induced by cysteamine and N-acetylcysteine. *Biochem. Pharma.* 37:881-888, (1988).

81. Meister, A., Anderson, M.E. and Hwang, O., Intracellular cysteine and glutathione delivery systems. *J. Amer. Col. Nutr.* 5:137-151, (1986).
82. Tsuda, H., Moore, M., Asamoto, M., Inoue, T., Ito, N., Satoh, K., Ichihara, A., Nakamura T., Amelizad, Z., and Oesch, F., Effect of Modifying Agents on the Phenotypic Expression of Cytochrome P-450, Glutathione S-Transferase Molecular Forms, Microsomal Epoxide Hydrolase, Glucose-6-phosphate Dehydrogenase and γ -glutamyltranspeptidase in Rat Liver Preneoplastic Lesions. *Carcinogenesis* 9: 547-554, (1988).
83. Baliga, B.S., Pronczuk, A.W. and Munro, H.N., Mechanism of Cycloheximide Inhibition of Protein Synthesis in a Cell-free System prepared from rat liver. *J. Biol. Chem.* 244:4480-4489, (1969).
84. Tateishi, N., Higashi, T. Shinya, S. Naruse, A. and Sakamoto, Y., Studies on the regulation of glutathione level in rat liver. *J. Biochem.* 75:93-103, (1974).
85. Gravela, E., Poli, G., Albano, E., and Dianzani, M., Studies on Fatty Liver with Isolated Hepatocytes. *Experimental and Molecular Pathology* 27: 339-352, (1977).
86. Phelps, D.T., Deneke, S.M., Baxter, D.F., and Fanburg, B.L., Erythrocytes Fail to Induce Glutathione in Response to Diethyl Maleate or Hyperoxia. *The American Physiological Society* 1040-0605: L272-276, (1989).
87. Tewari, S., Duerbeck, N., Ross-Duggan, J., and Noble, E., In Vitro Protein Synthesis by Inner Membranes of Rat Brain Mitochondria. *Research Communications in Chemical Pathology and Pharmacology* 22: 385-400, (1978).
88. Satav, J., Katyare, S., Fatterpaker, P., and Sreenivasan, A., Study of Protein Synthesis in Rat Liver Mitochondria: Use of Cycloheximide. *Eur. J. Biochem.* 73: 287-296, (1977).
89. Kosower, N., Vanderhoff, G. and Kosower, E.M., The Effects of glutathione disulfide on initiation of protein synthesis. *Biochimica Et Biophysica ACTA* 272:623-637, (1972).

90. Zehavi-Willner, T., Kosower, E.M., Hunt, T. and Kosower, N., The effects of the thiol-oxidizing agent diamide on initiation and translation in rabbit reticulocytes. *Biochimica Et Biophysica ACTA* 228:245-251, (1971).
91. Aab:oth, G., Gimes, G., Hertelendy, F. and T:oth, M., The relation between thromboxane and prostaglandin synthesis in human decidua tissue. *Biochim Biophys. Acta.*1002(1):101-108. Mar 14, (1989).
92. Mimata, H., Ogata, J. and Takeshita, M., Regulation of prostaglandin synthesis by reduced glutathione in urinary bladder epithelium. *J. Urol.* 139:616-620, (1988).
93. Imokawa, G., Analysis of initial melanogenesis including tyrosine transfer and melanosome differentiation through interrupted melanization by glutathione. *J. Invest. Dermatol.* 93:100-107, (1989).
94. Vandenberghe, Y., Ratanasavanh, D., Glaise, D., and Guillouzo, A., Influence of Medium Composition and Culture Conditions on Glutathione S-Transferase Activity in Adult Rat Hepatocytes During Culture. *In Vitro Cellular & Developmental Biology* 24: 281-288, (1988).